Radiative Transfer and Regional Climate Change

***Kuo-Nan Liou**
Joint Institute for Regional Earth System Science and Engineering (JIFRESSE) and Atmospheric and Oceanic Sciences Department
University of California, Los Angeles, CA, USA

***With contributions from Y. Takano, W. L. Lee, Y. Gu, Z. Liu, Q. Li, R. Leung, P. Yang, and T. Fickle. Research work supported in part by NSF and DOE.**

- **Evidence of Mountain Snowmelt and Climate Change**
- **BC and Snow Cover Reduction in the Tibetan Plateau**
- **Some Evidence of Snow Albedo Reduction in the Sierras**
- **Radiative Forcing by BCs (Aggregates)**
- **3D Mountain/Snow Effects on Surface Solar Fluxes**
- **The Concept of Aerosols/Mountain-Snow/Albedo Feedback**
- **Connection to WRF and the Community Land Model (CLM), and Summary**

IRC Symposium, Berlin, Germany, August 9, 2012

Kyetrak Glacier, Tibet

Rongbuk Glacier, Tibet

Mount Kilimanjaro, Tanzania

Qori Kalis Glacier, Peru (World Data center for Glaciology)

Strong Evidence for Global Warming; however, absorbing aerosols have also contributed to and amplified the retreat of glaciers.

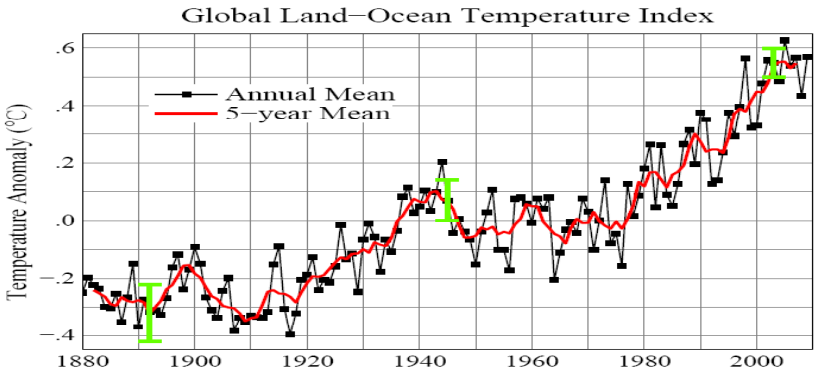

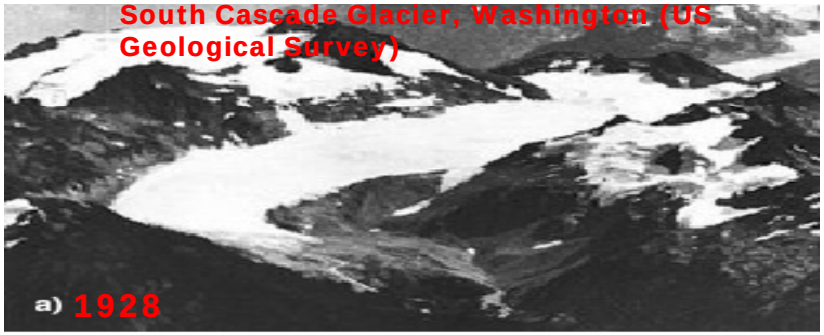

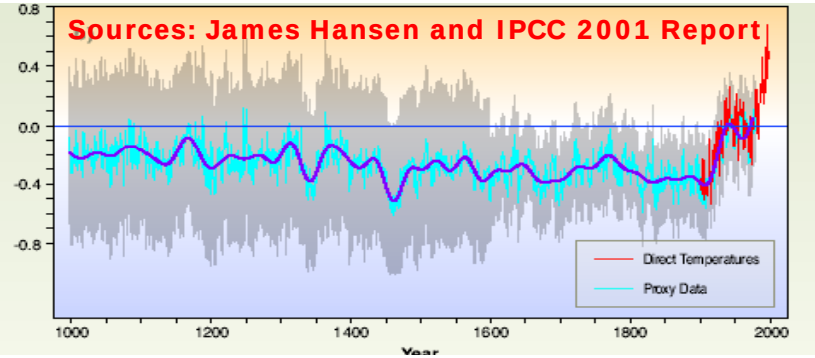

(a) NH March-April average snow-covered area (Brown 2000) and NOAA satellite data set. The smooth curve shows decadal variations, and the shaded area shows the 5 to 95% range of the data estimated after first subtracting the smooth curve. (b) Differences in the distribution of NH March-April average snow cover between earlier (1967–1987) and later (1988–2004) portions of the satellite era. Negative values indicate greater extent in the earlier portion of the record. Red curves show the 0 and 5^0 C isotherms averaged for March and April 1967 to 2004 (after IPCC 2007).

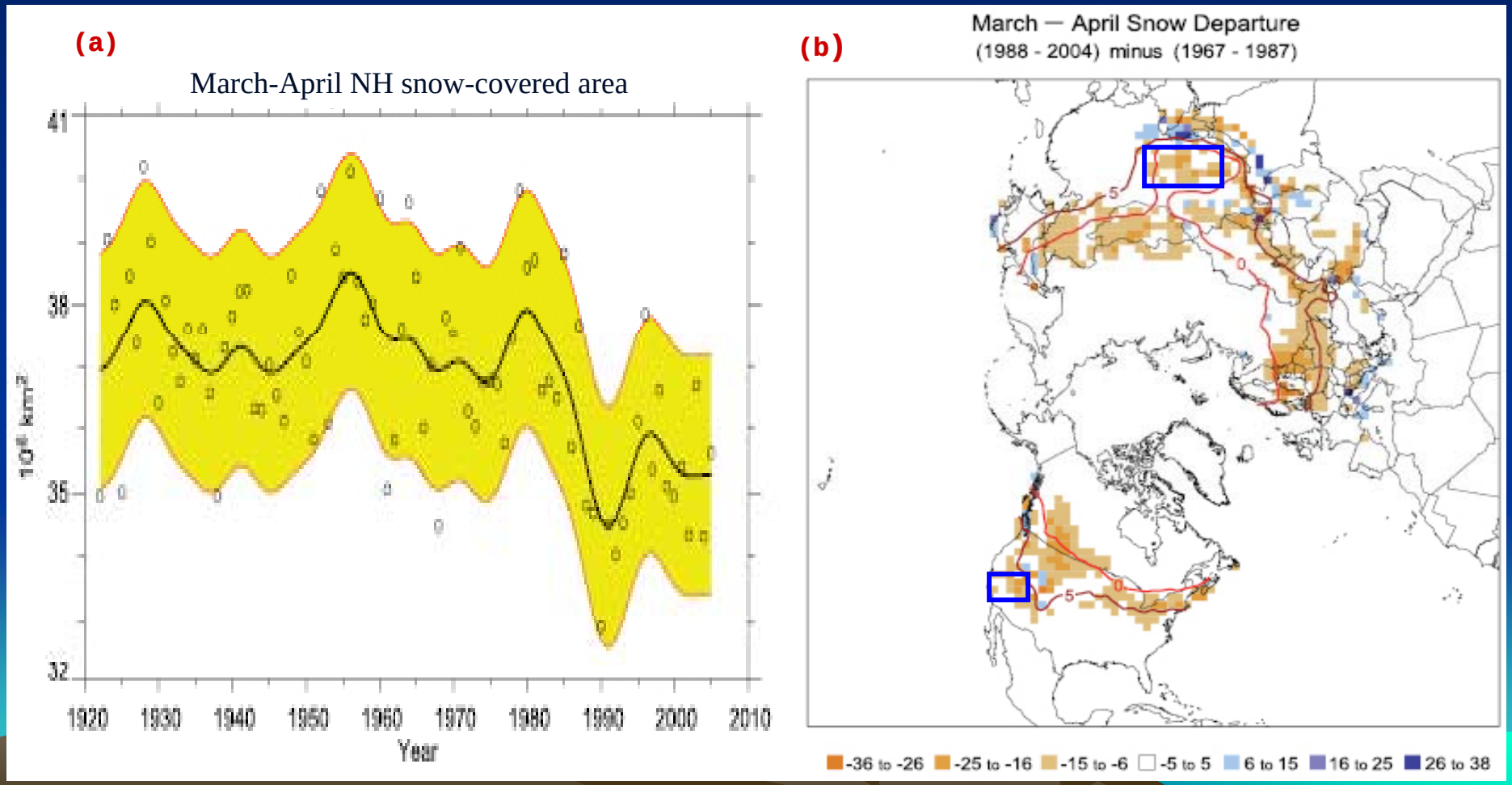

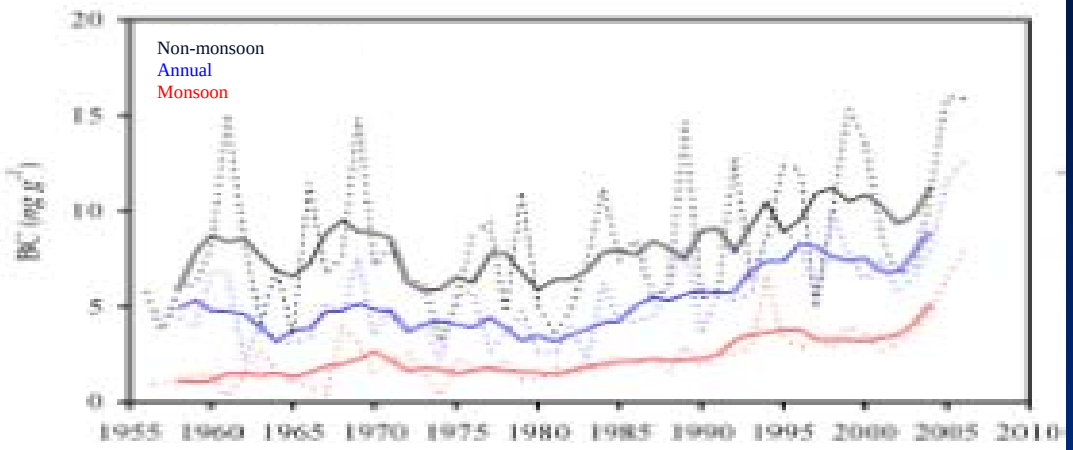

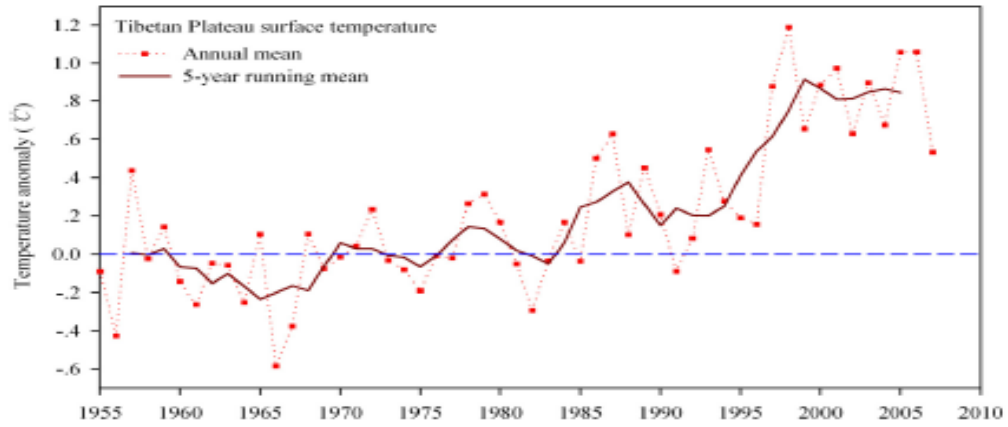

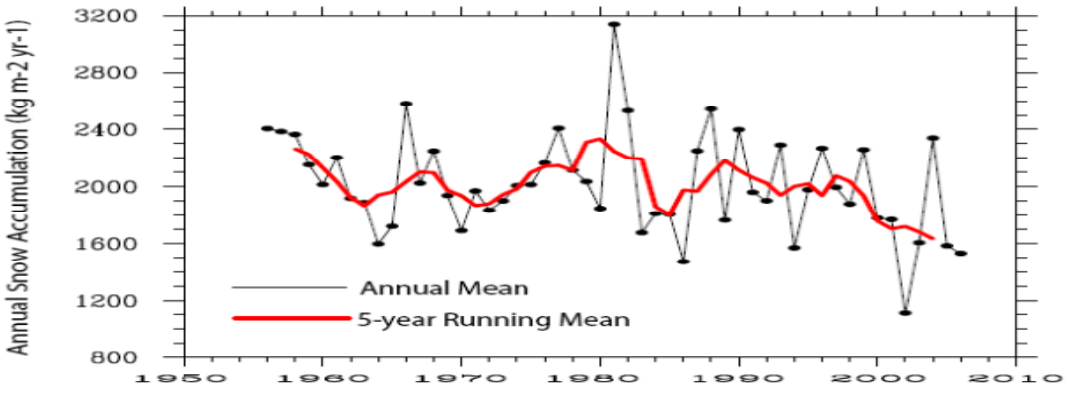

Top: Black carbon concentration (ng/g) determined at the Zuoqiupu Glacier of the Tibetan Plateau from 1955 to 2005. Shown are annual and 5-year running mean results for non-monsoon, monsoon (lower due to high precipitation rate), and annual cases. The BC source is Asia, primarily the Indian subcontinent.

Middle: Surface air temperature anomaly in terms of annual and 5-year mean on the Tibetan Plateau relative to 1951-1980 mean, averaged over the area with altitude greater than 4,000 m above sea level.

Bottom: Annual snow accumulation on the Zuoqiupu Glacier (kg/m2/yr) from 1956 to 2006 along with 5-year running mean results, revealing reduction since 1990 (after Xu et al. 2009).

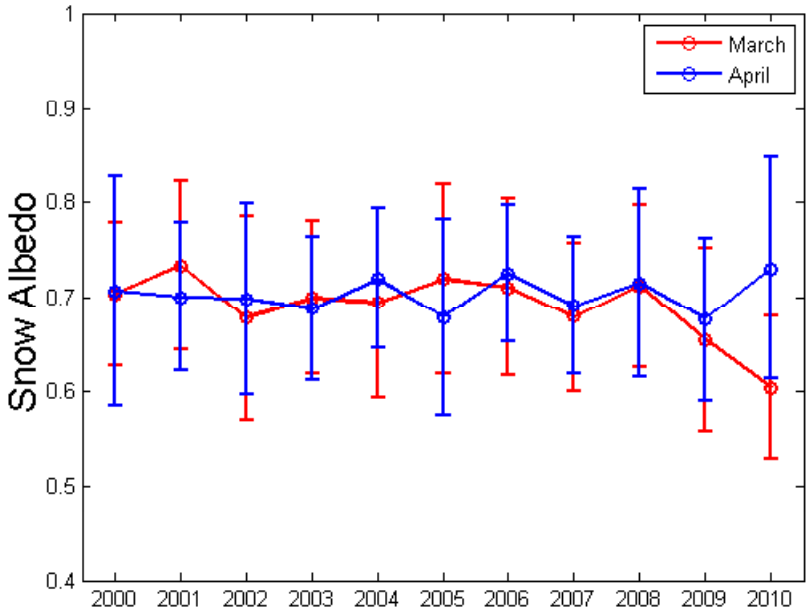

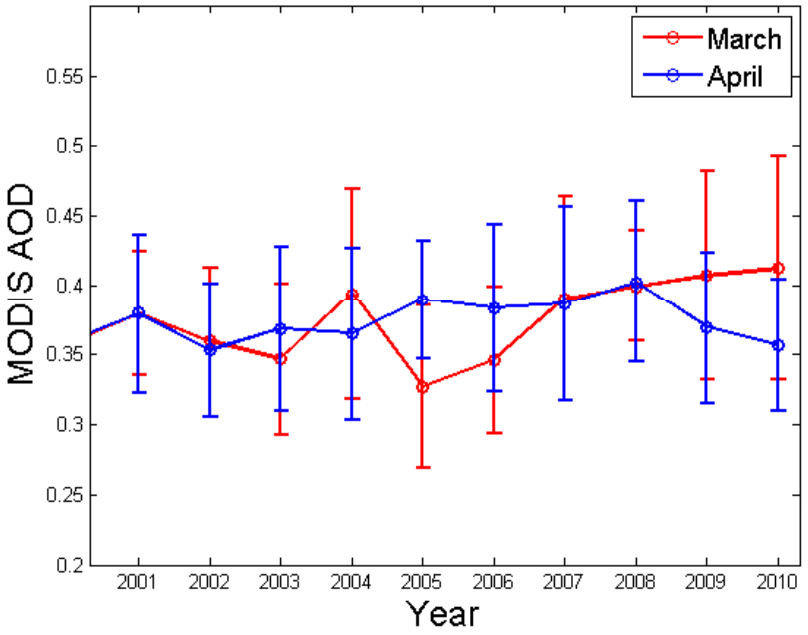

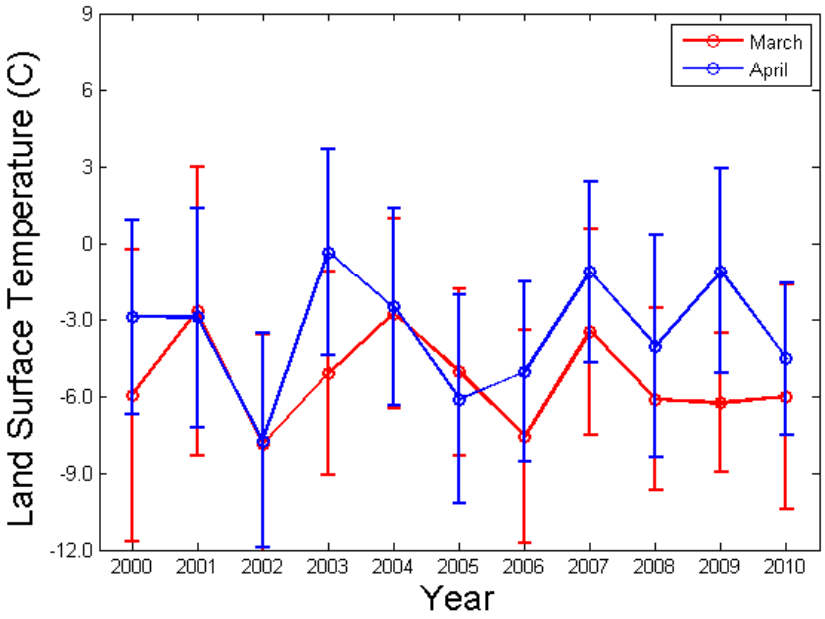

Monthly averages of snow albedo for pixels with 100% snow cover, land surface temperature, and aerosol optical depth over the Tibetan Plateau in March and April from 2000 to 2010 taken from the MODIS data products. Error bars indicate one standard deviation (paper in preparation).

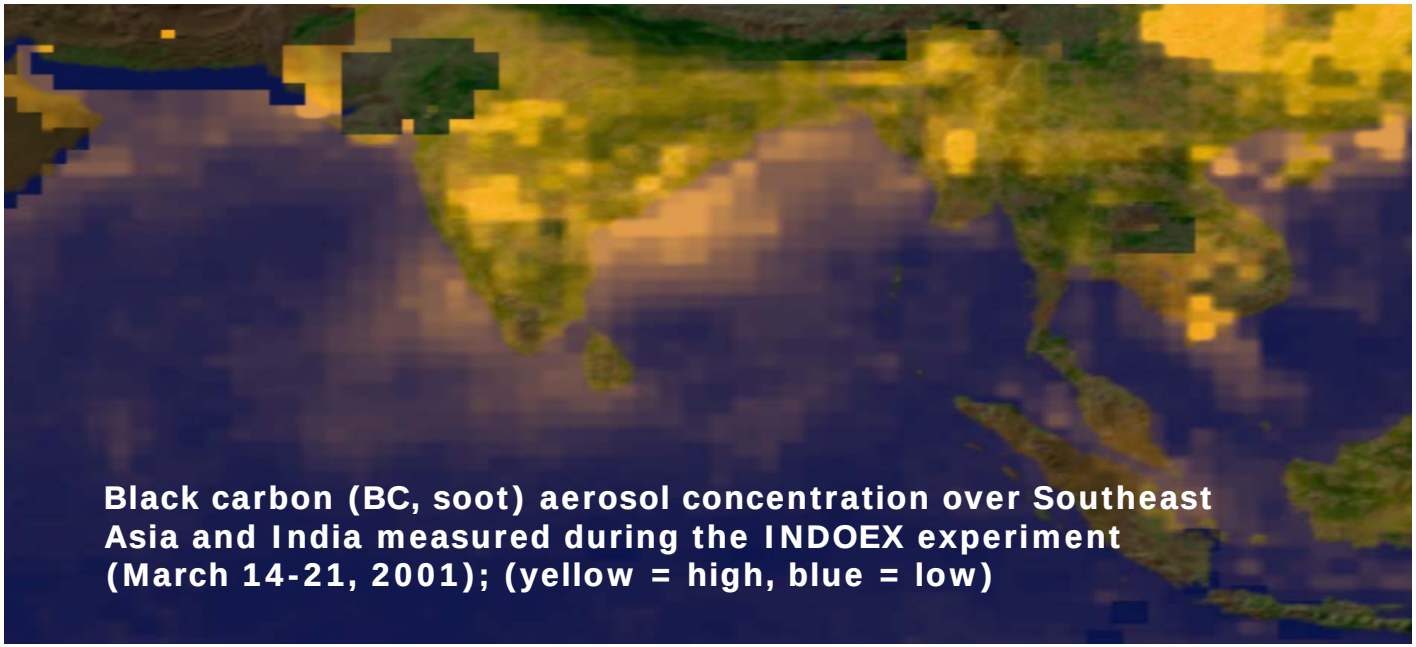

Black carbon (BC, soot) aerosol concentration over Southeast Asia and India measured during the INDOEX experiment (March 14-21, 2001); (yellow = high, blue = low)

"2001 Perfect Dust Storm"

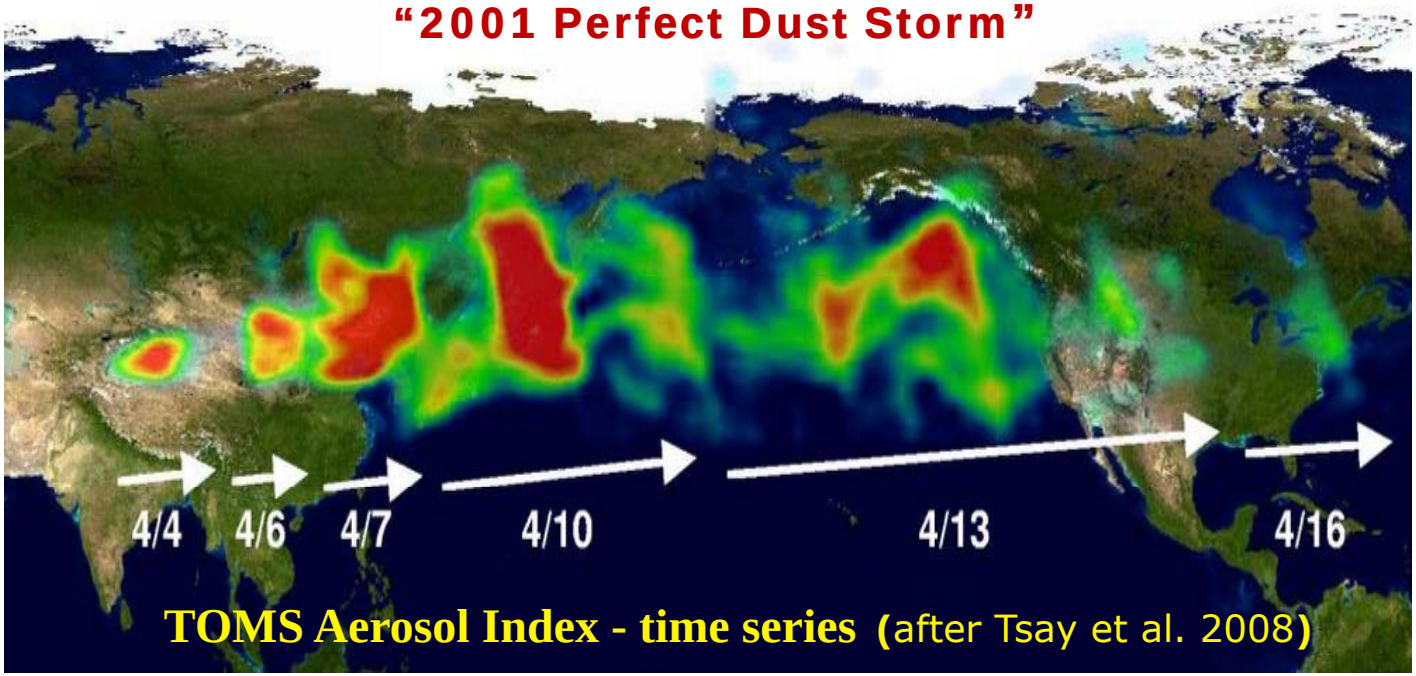

TOMS Aerosol Index - time series (after Tsay et al. 2008)

Aerosol optical depths determined from MODIS of NASA satellites for March and April 2000-2009, a 10 year period, illustrating the transport of absorbing aerosols from China and Southeast Asia across the Pacific to the United States (only 4 years are shown; courtesy of W. L. Lee, Academia Sinica).

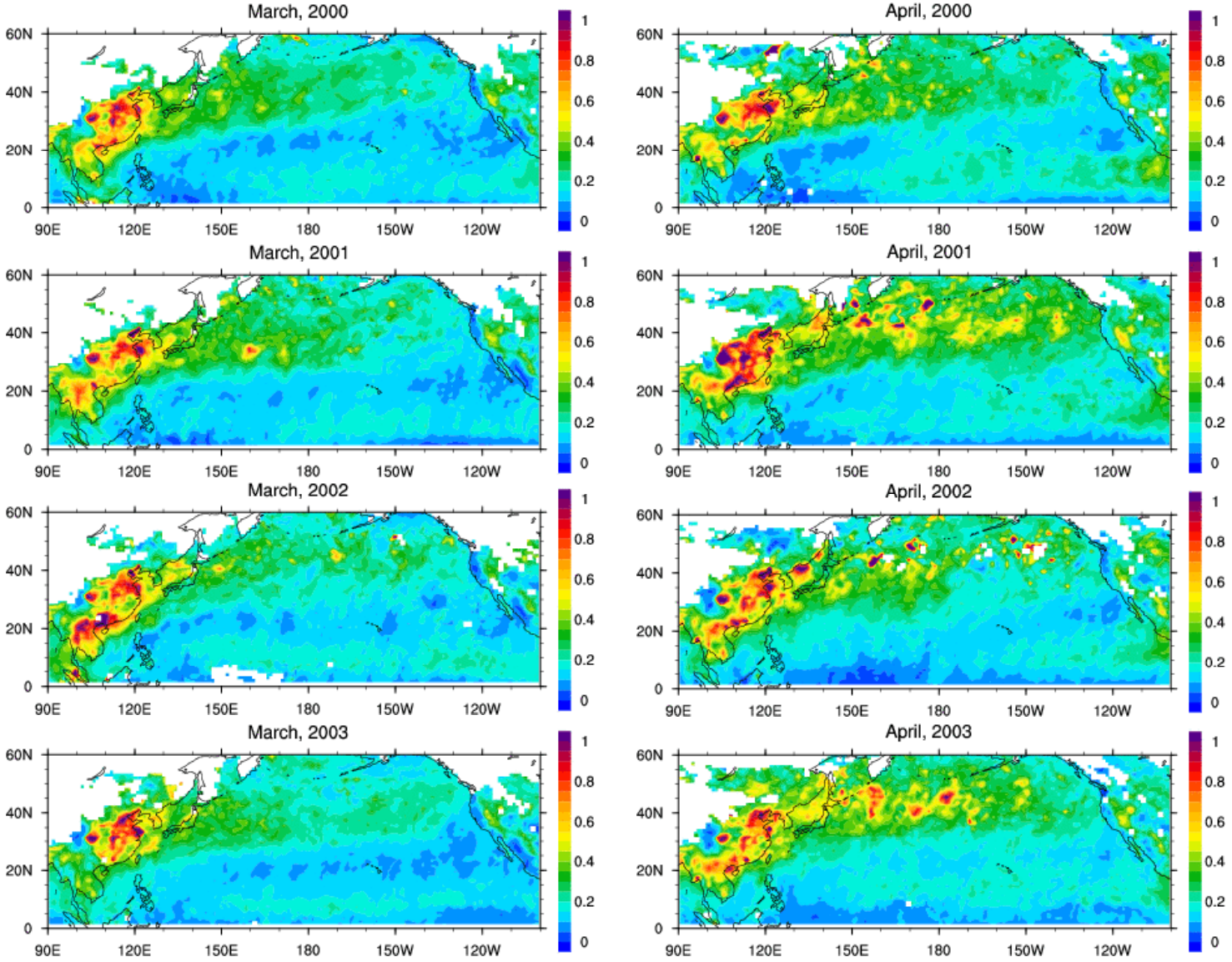

Total aerosol optical depths for March and April 2006 simulated from a chemical transport model, illustrating the effects of absorbing aerosols generated in China on the west coast of the United States (courtesy of Q. Li, UCLA).

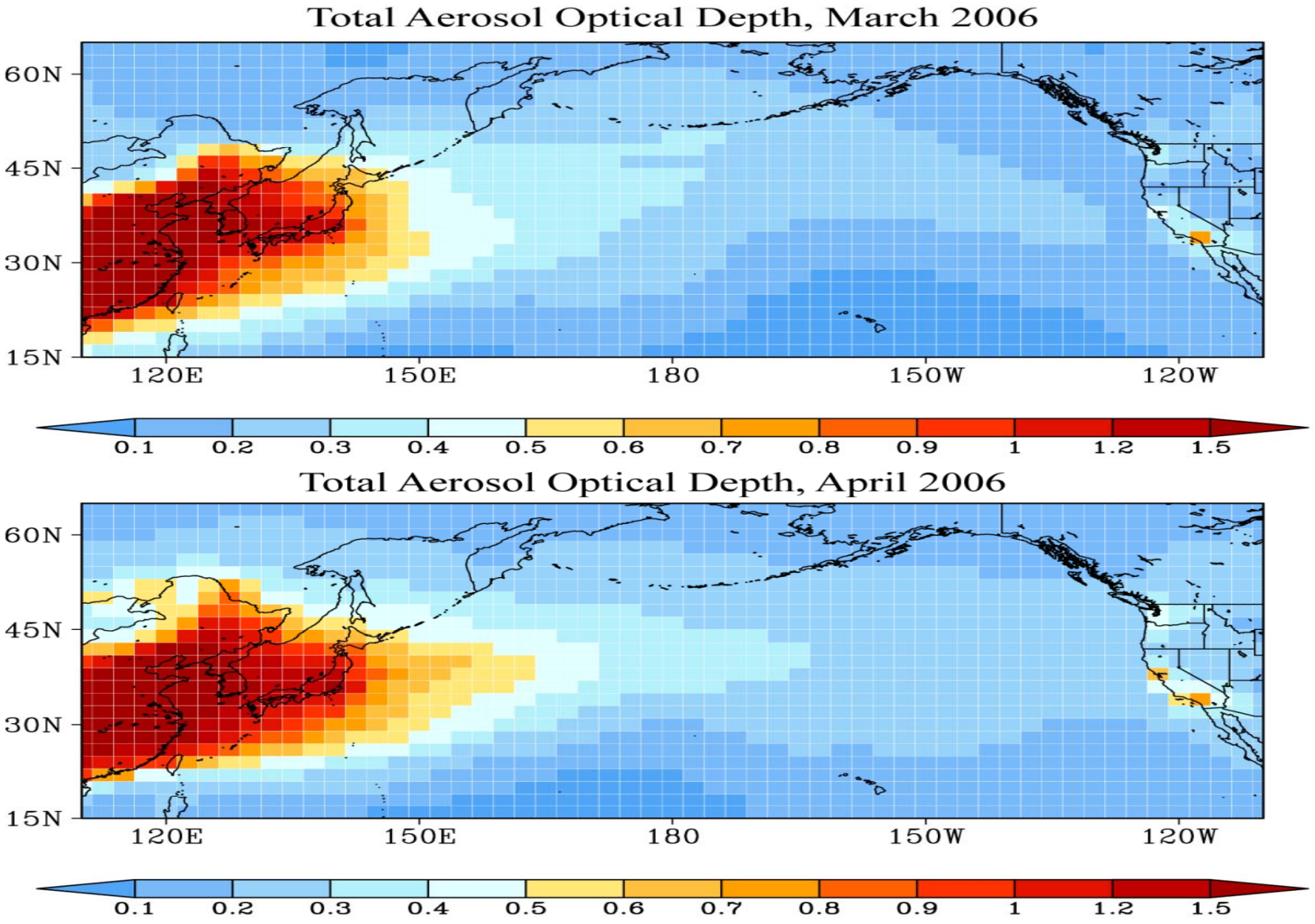


Northern California (local)
Southern California (local)


Sierra Nevada (America)
BC/Dust-Snow Impact on
Regional Climate


Rocky (America)

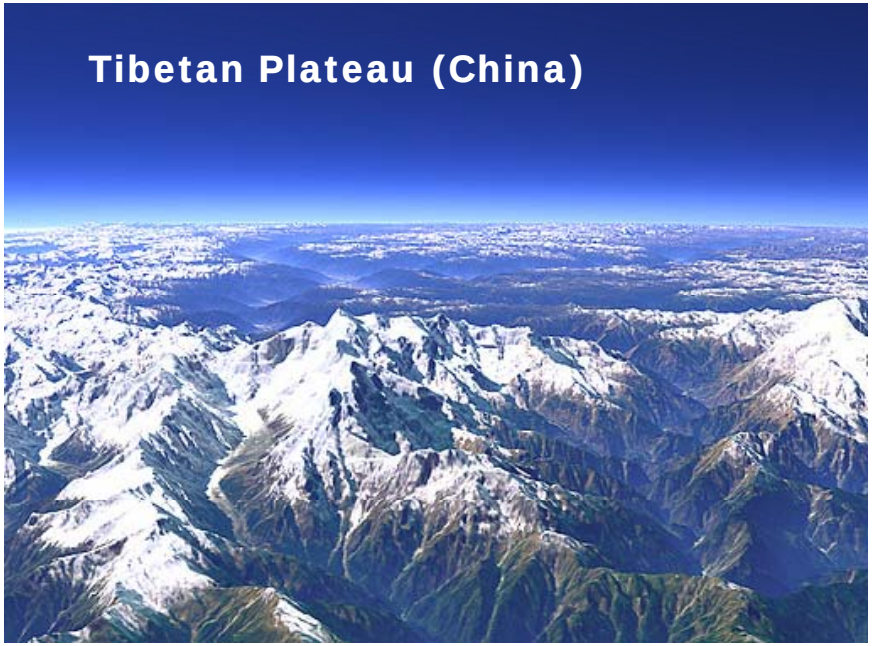
Tibetan Plateau (China)


Alps (Europe)

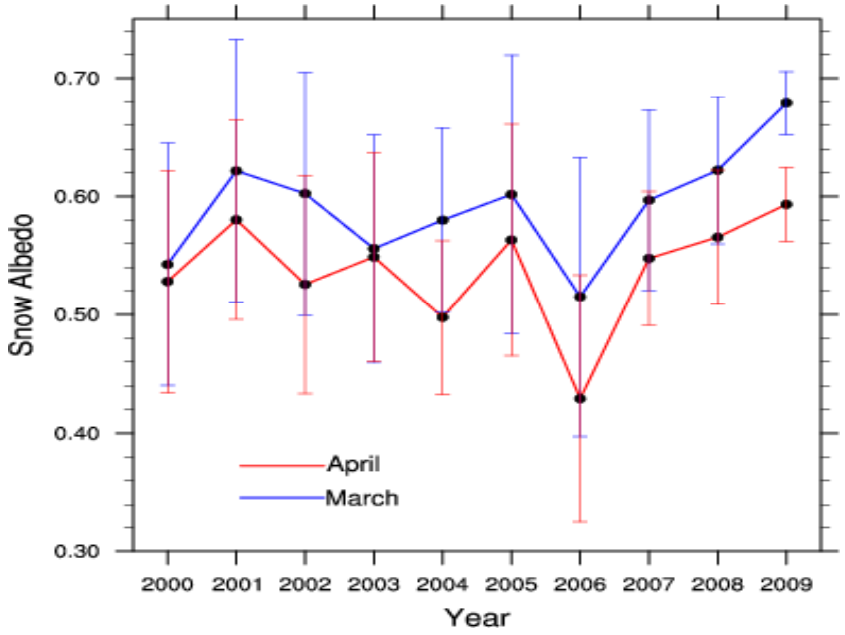

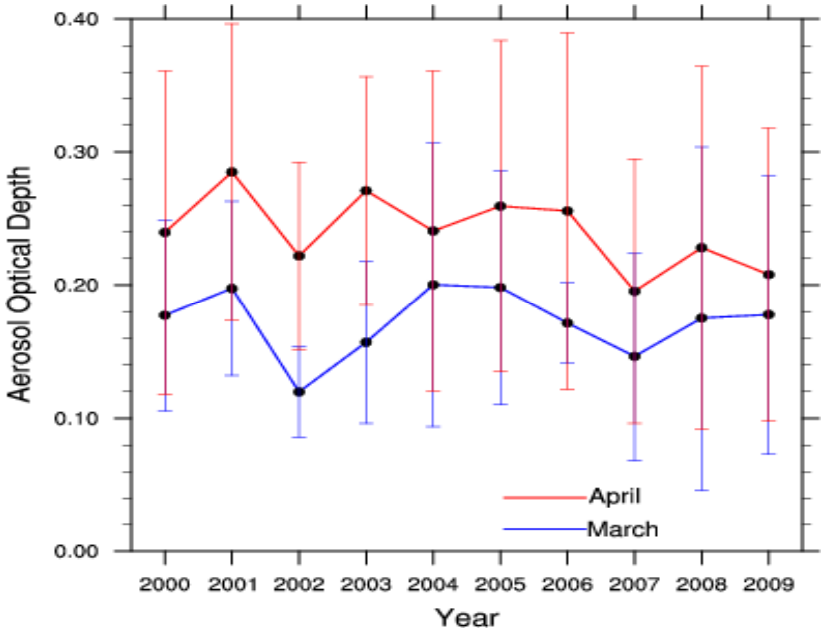

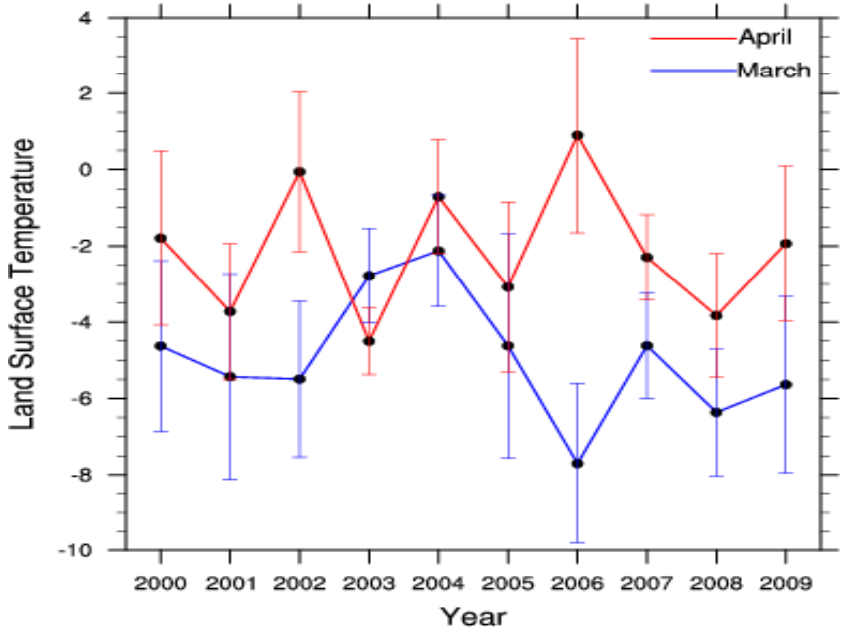

Monthly averages of snow albedo for pixels with 100% snow cover, land surface temperature and aerosol optical depth over the Sierras in March and April from 2000 to 2009. Error bars indicate one standard deviation. A significant negative correlation between snow albedo and aerosol optical depth: $a = 0.56-0.038T-0.026\tau$ (Lee and Liou 2012, Atmo. Env.).

Light Absorption & Scattering by BC / Dust

BC: Highly Absorbing
Dust: Absorbing & Scattering

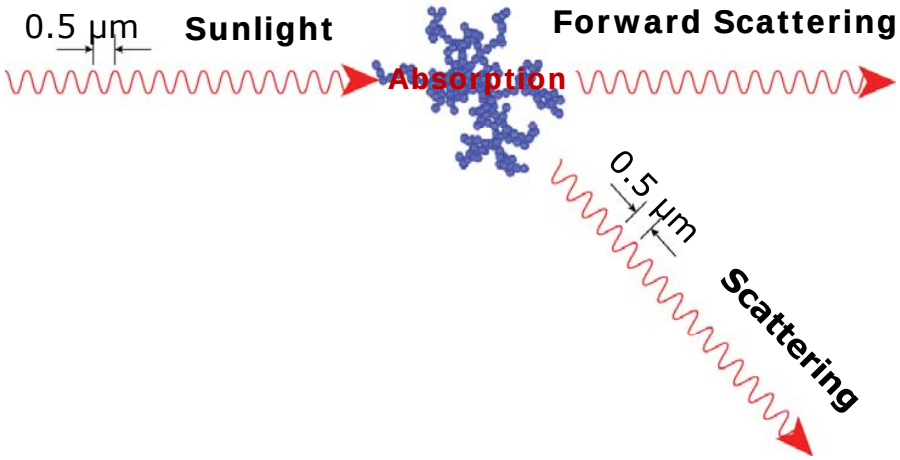

Absorption: Transform to Heat

Scattering: Redirect the energy in different directions

Direct Radiative Forcing & Regional Climate

Absorption of Sunlight by BC / Dust

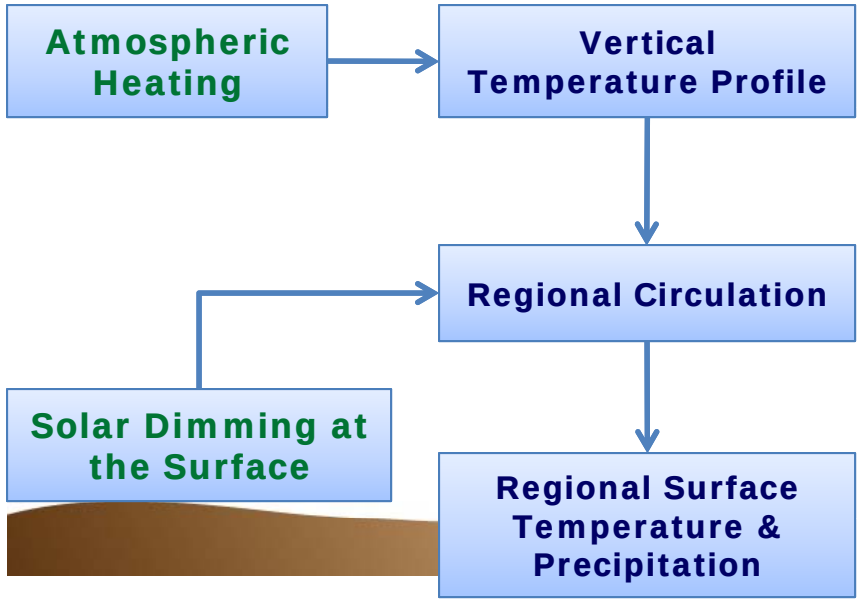

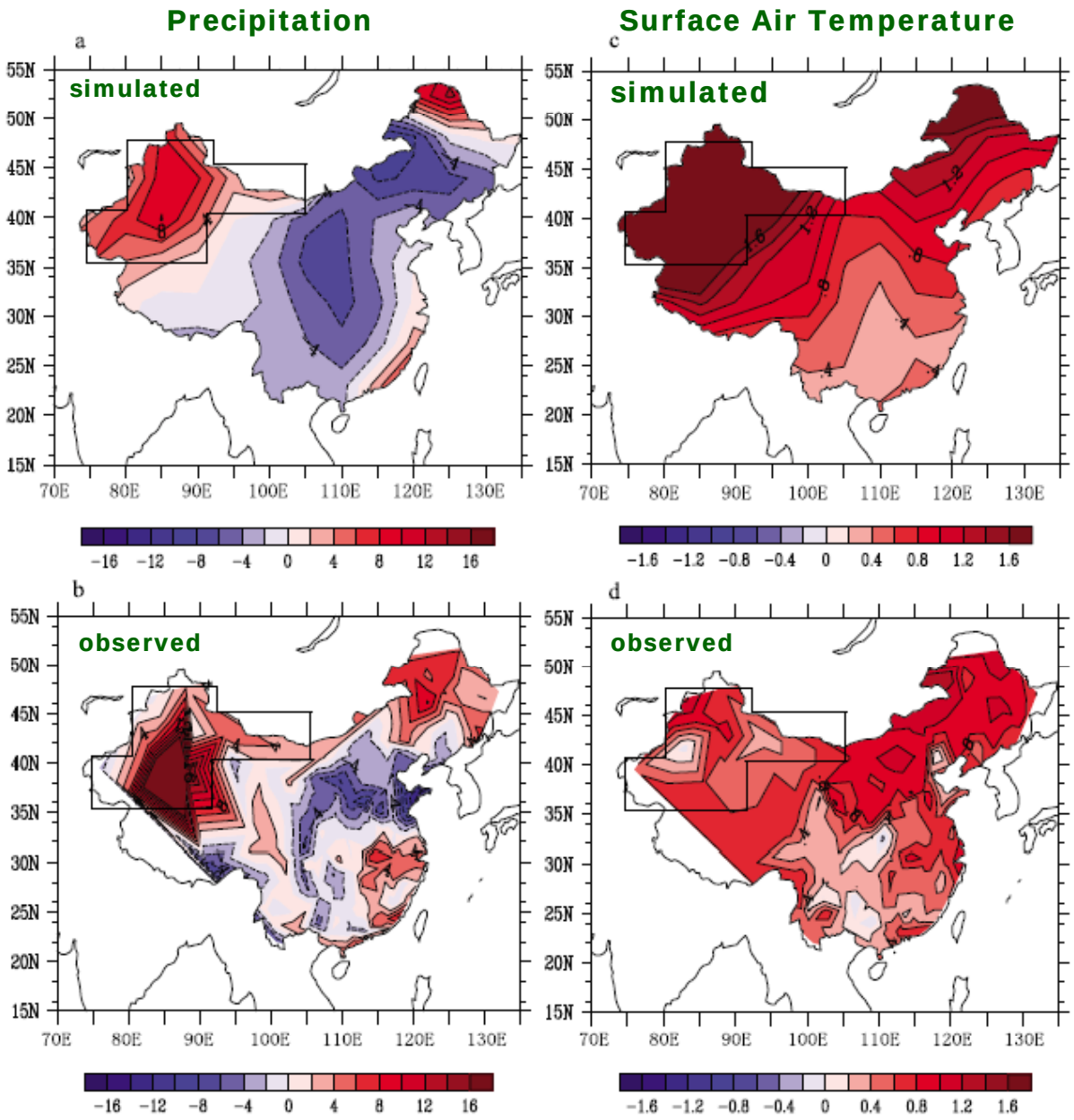

Simulated annual mean differences in (a) precipitation (%) and (c) surface air temperature (K) between Experiments B and A, along with the observed (b) precipitation (%) and (d) surface air temperature anomalies (K) over China in the1990s. Exp A consists of 10% BC and 90% non-absorbing aerosols (ω = 0.92). Exp B consists of 15% BC and 85% of non-absorbing aerosols (ω =0.88). The sea surface temperature, greenhouse gases, and other forcings are fixed in these two experiments so that aerosols are the only forcings in 5-year simulations (after Gu, Liou et al. 2010).

Light Scattering and Absorption by Dust and Black Carbon: Fundamental to the Understanding of Aerosol Climate Forcings

Dust

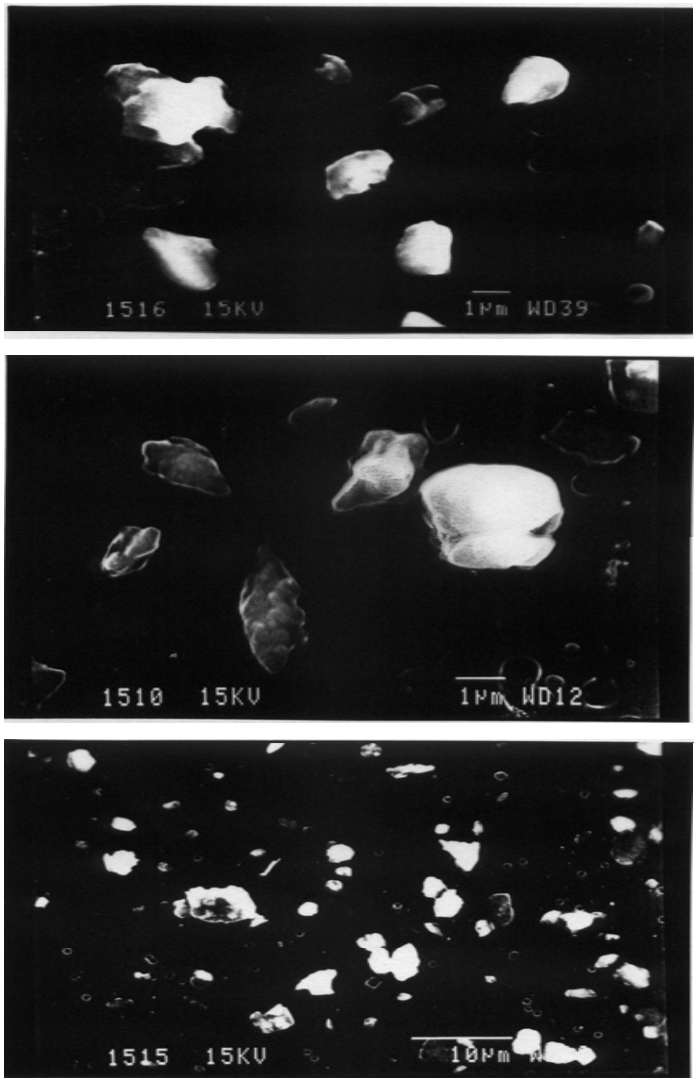

Black Carbon

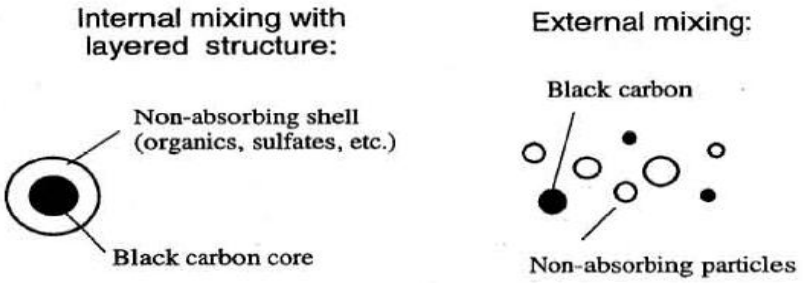

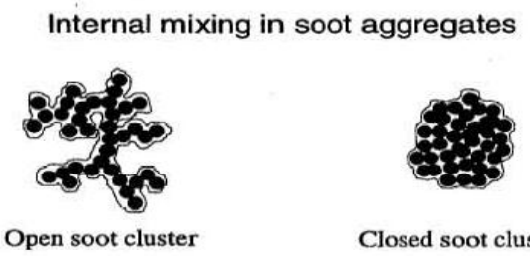

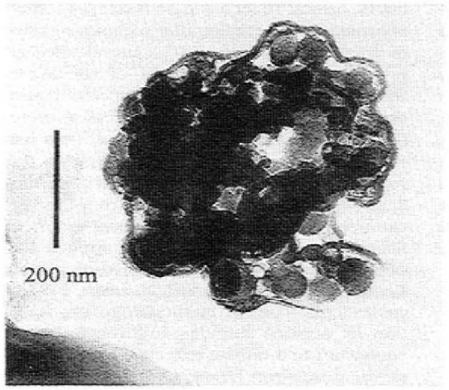

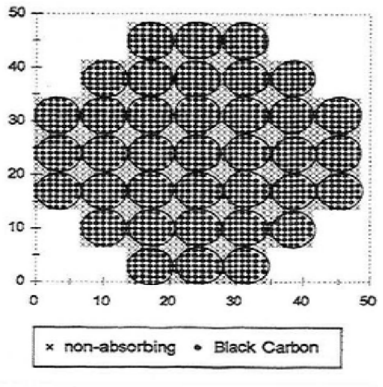

Construction of aggregates based on stochastic processes using homogeneous and shell spheres (smooth and irregular) as building blocks (Liou et al. 2010, 2011): closed and open cells, and observed soot.

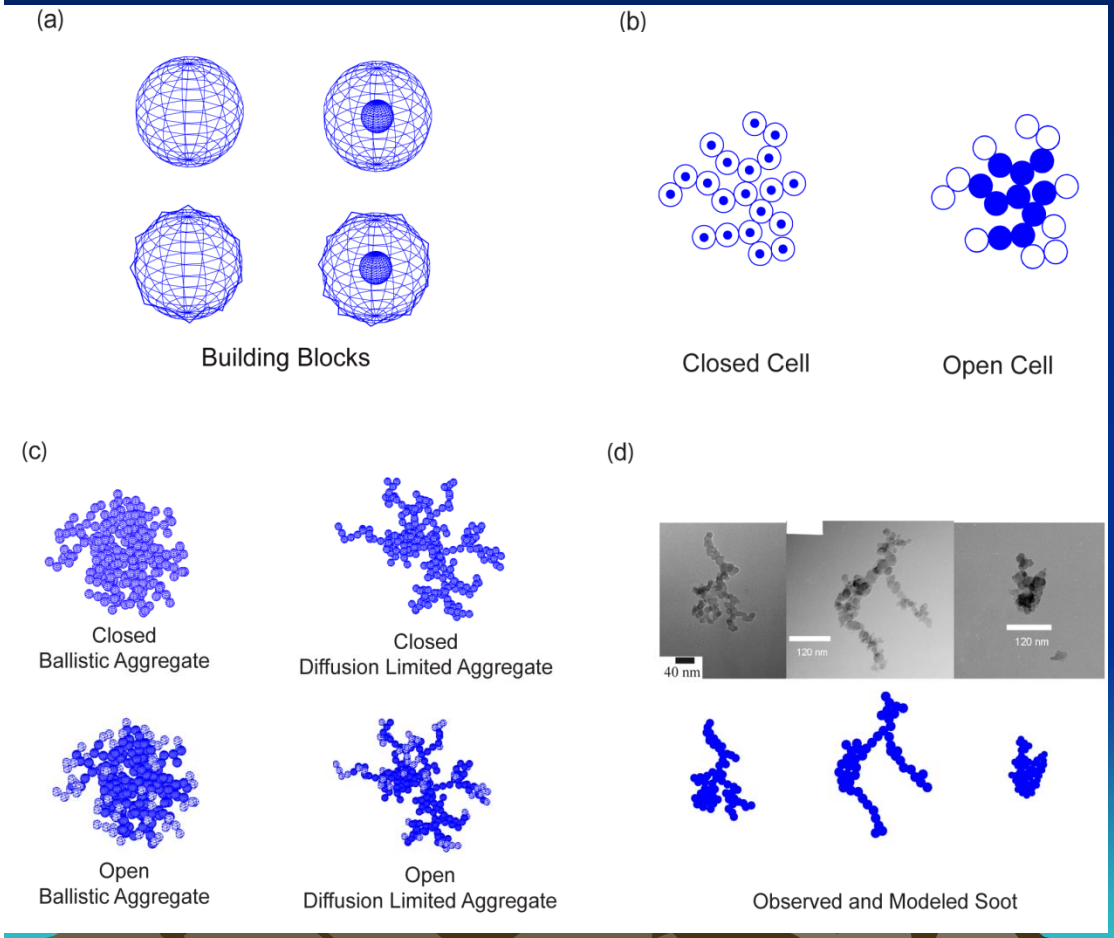

Light absorption and scattering by small irregular particles based on the geometric-optics and surface-wave approach verified by comparison with existing results for columns and plates (Liou, Takano and Yang 2011).

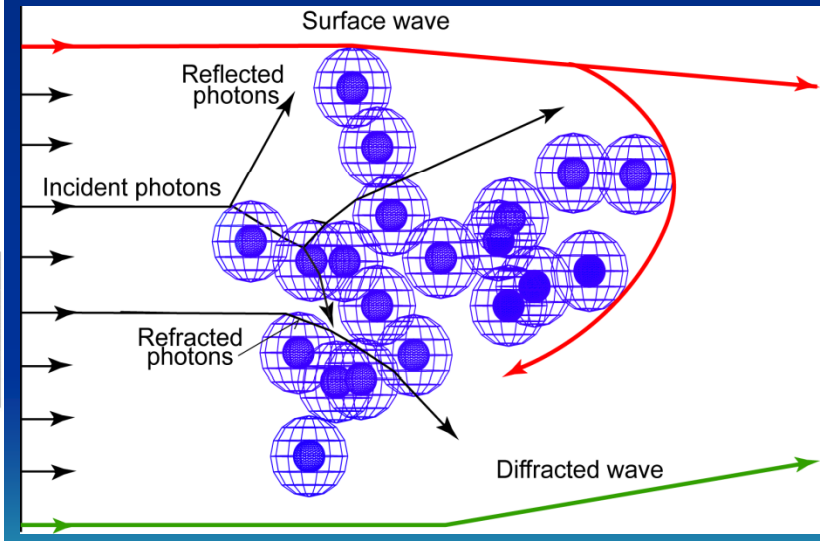

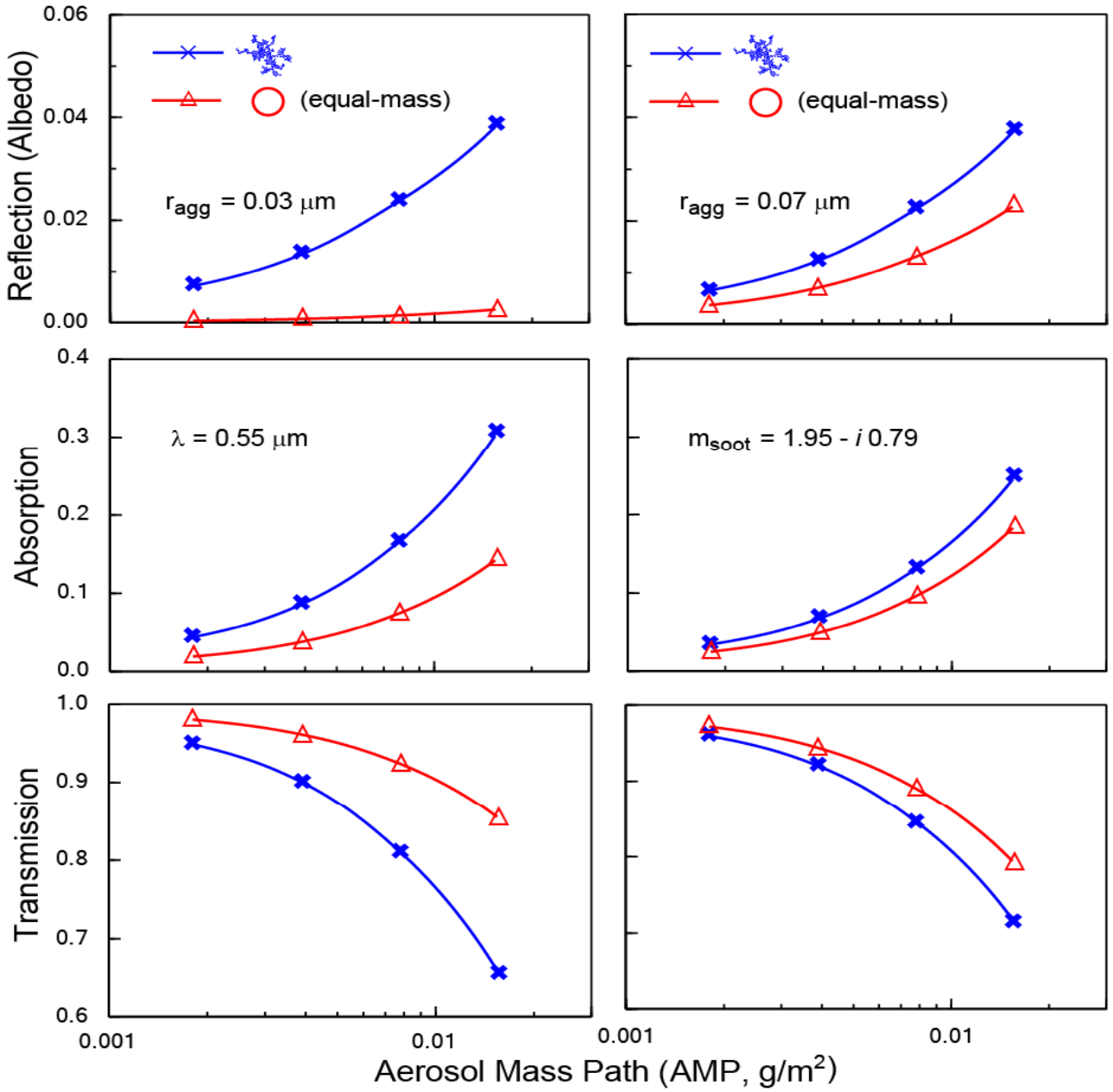

Reflection (Albedo), absorption, and transmission for a soot layer as a function of aerosol mass path (AMP) on a black surface using a solar zenith angle of 60^0. The 0.03 μm radius is the mean observed equivalent radius for BC aerosols. Note: substantial differences between the two BC shapes using diffusion limited aggregate and equal-mass (and equal-volume) spheres. Optical depth τ can be obtained by τ = a_e AMP, where a_e is the specific extinction coefficient (m^2/g). The adding-doubling method was used for radiative transfer calculations.

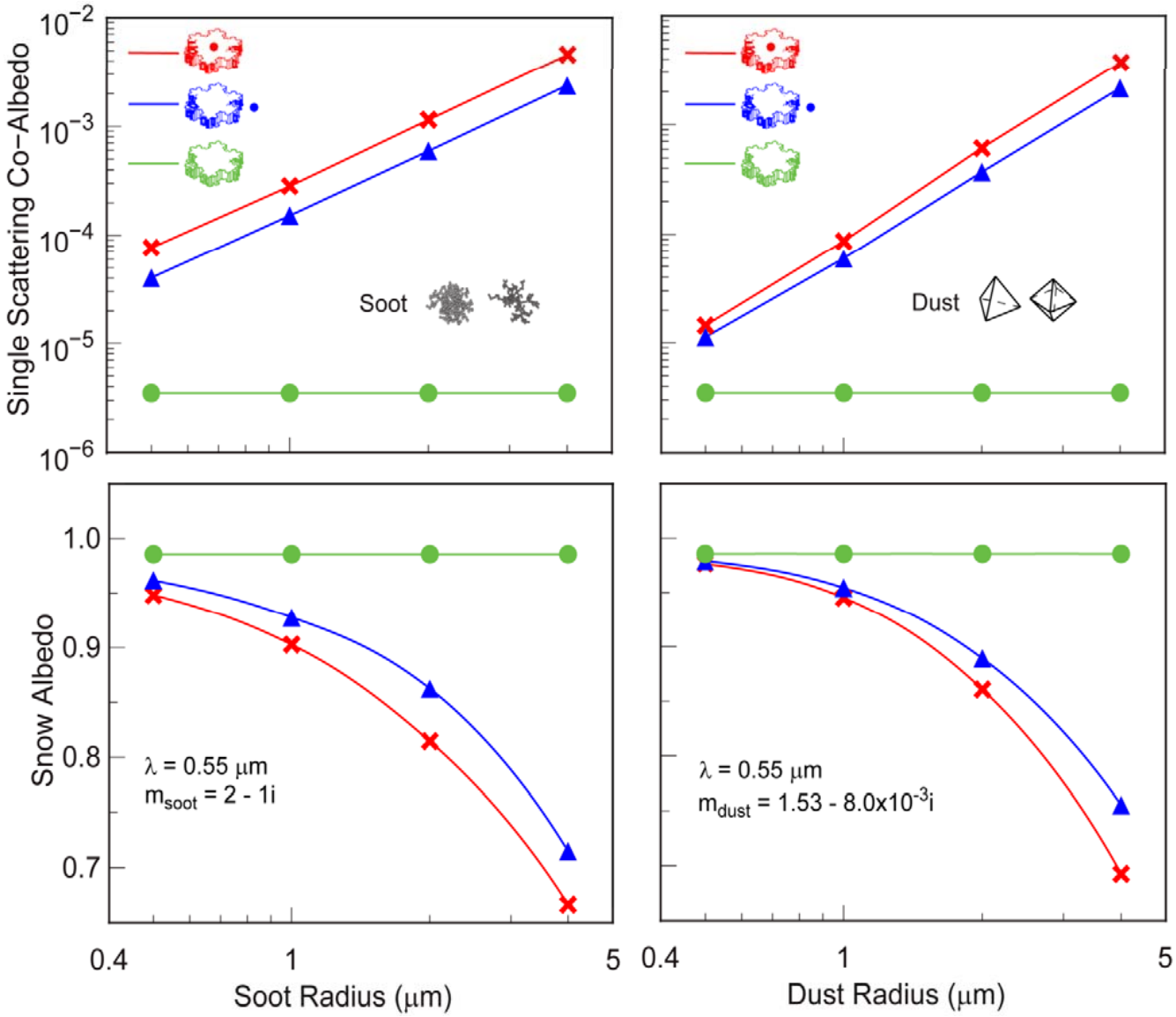

Visible single-scattering co-albedo (the ratio of absorption and extinction coefficients) and snow albedo as a function of soot and dust equivalent radii for a snow grain of 50 μm in equivalent radius for pure and contaminated conditions (μ_0 = 0.5 and optically semi-infinite snow layer). Large differences in snow albedo are shown with external and internal mixing cases. A 1 μm soot particle internally mixed with snow grains could effectively reduce snow albedo as much as 5-10 % (Liou et al. 2011).

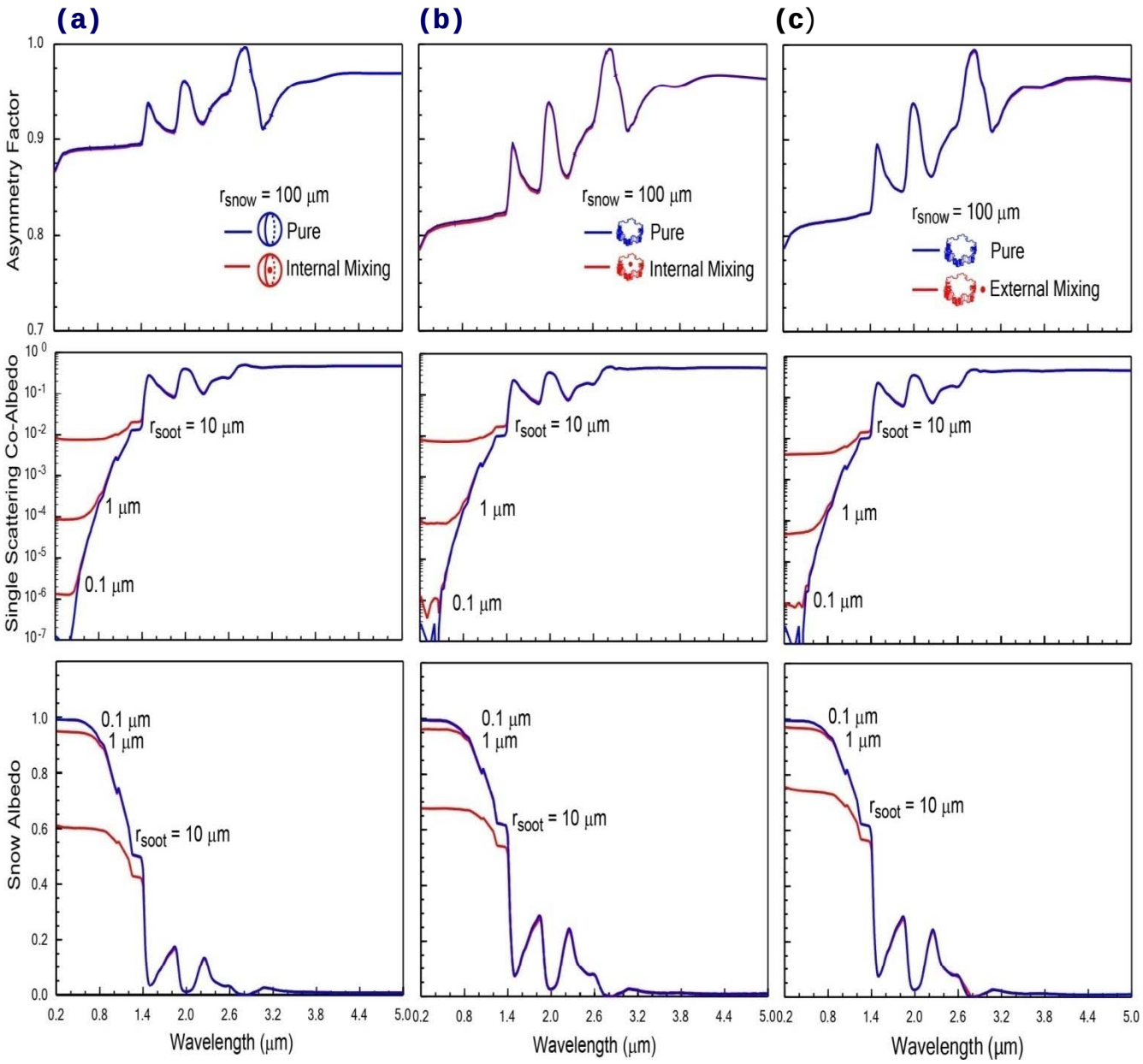

The effect of internal and external mixings in snow grains and spherical assumption on the asymmetry factor (upper panel), single-scattering co-albedo (middle panel) and snow albedo (μ_0 = 0.5, optically semi-infinite layer; lower panel) covering 0.2 to 5μm solar spectrum. The snow grain size is 100 μm with 3 BC sizes of 0.1, 1, and 10 μm. (a) Sphere (asymmetry factor), and (b) and (c) internal and external mixing (single scattering albedo). For application to CLM-WRF, total BC deposition can be converted to a mean BC size.

3D Radiative Transfer (Monte Carlo Photon Tracing) in Mountains: 10-30 W / m² in Regional Surface Energy Balance (Liou et al. 2007; Lee et al. 2011, regression parameterization for use in WRF-CLM)

Solar radiation:

- Direct: solar incident angle θ_i
- Diffuse: sky view factor V_d
- Direct reflected: terrain configuration factor C_t
- Diffuse reflected: terrain configuration factor C_t
- Coupled: terrain configuration factor C_t

Thermal infrared radiation:

- Emitted in the atmosphere or from the surface
- Starting location sampled from a set of pre-divided cubic cells
- Random direction and isotropic emission (emissivity & temperature)

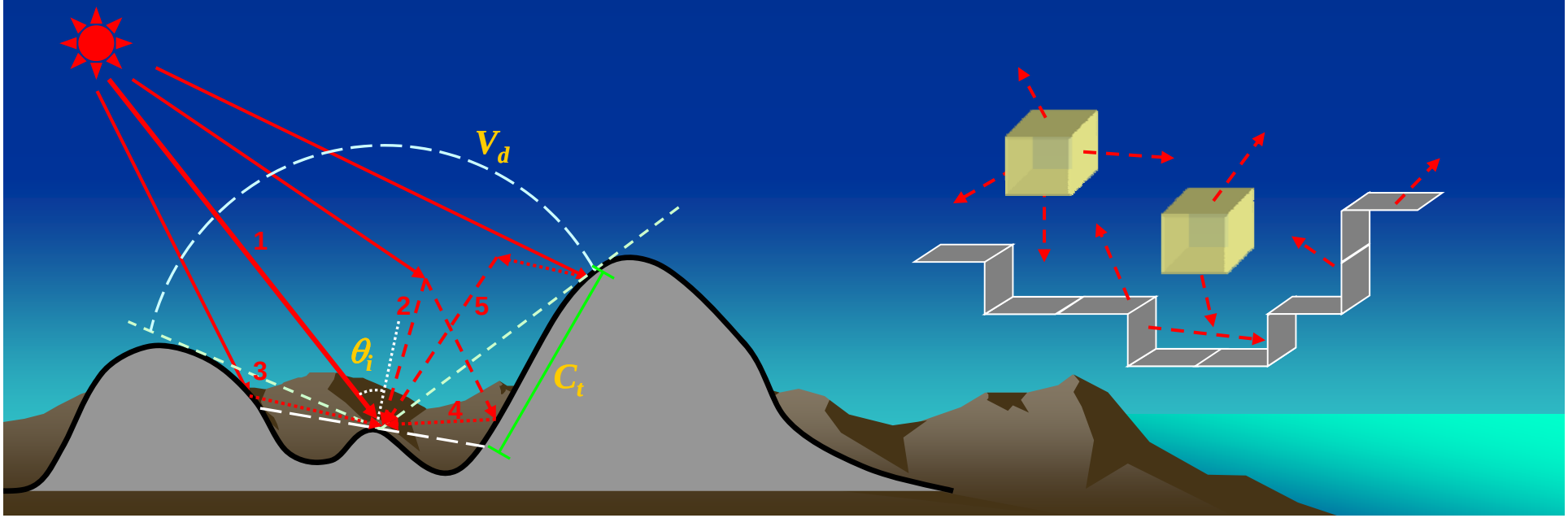

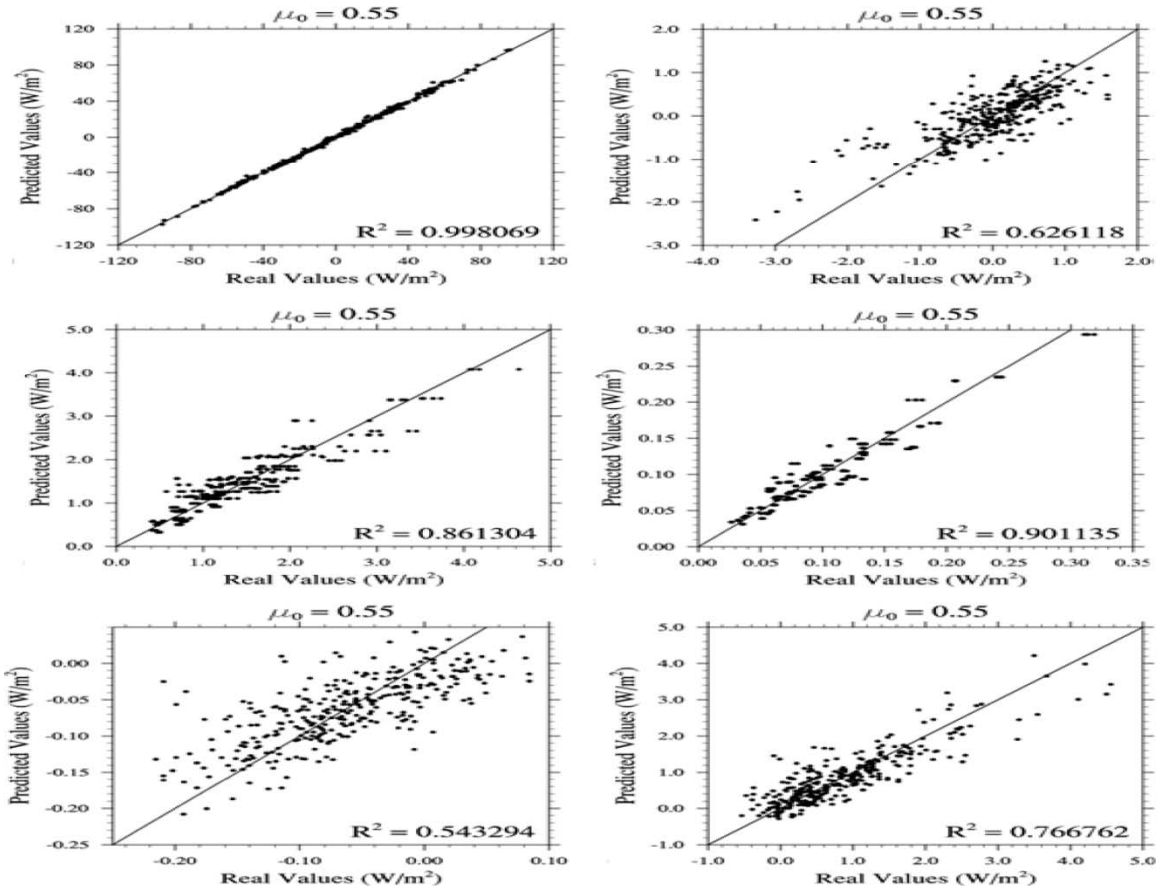

Comparison of the deviations of the five flux components computed from Monte Carlo simulations (real values) and multiple regression equations (predicted values). The upper panel is for direct (left) and diffuse (right) fluxes. The middle panel is for direct-reflected (left) and diffuse-reflected (right) fluxes. The lower panel shows the coupled flux with a surface albedo of 0.1 (left) and 0.7 (right). The most important component is direct flux (~ 700 W/m²), followed by direct-reflected flux (Lee et al. 2011).

We have derived 5 universal regression equations for flux deviations which have the following general form:

$$F^*_i = a_i + \Sigma\, b_{ij}\, y_j,\ i = \text{dir, dif, dir-ref, dif-ref, and coup,}$$

where a_i is the intercept, y_j is a specific variable, and b_{ij} are regression coefficients. For example, for the deviation of direct flux, we have $F^*_{dir} = a_1 + b_{11}\, y_1 + b_{12}\, y_2$, where y_1 is the mean cosine of the solar zenith angle and y_2 is the mean sky view factor. This parameterization is applicable to clear as well as cloudy conditions using cloud optical depth as a scaling factor.

Simulating 3D Radiative Transfer Effects Over the Sierra Nevada Mountains Using WRF: HYDRO 1km Geographic Data

Elevation (m)

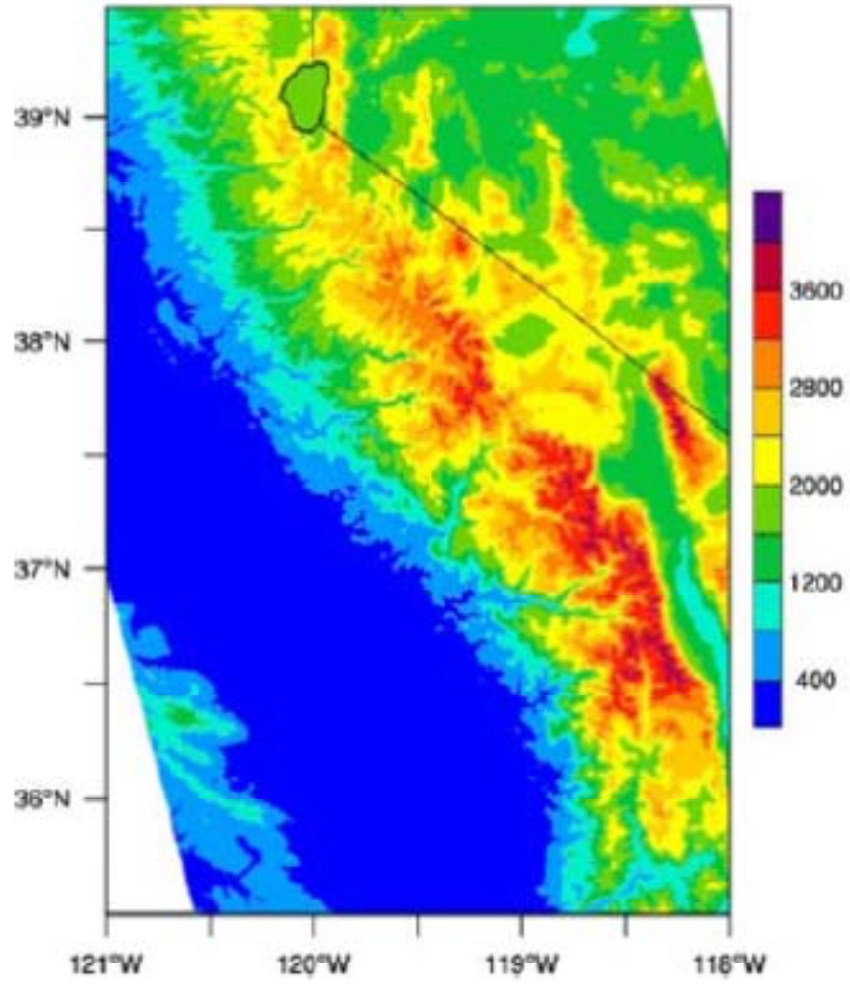

Slope (degree)

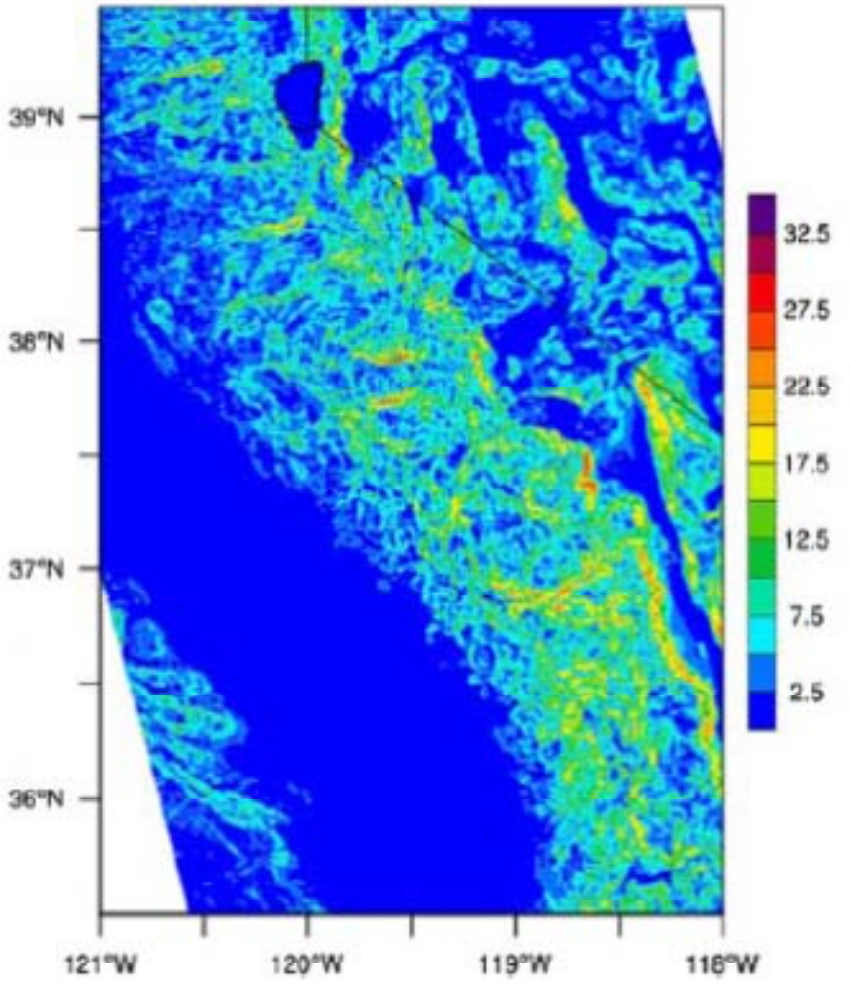

Solar Flux Differences (3D-PP, W/m²) for March 29, 2007 in WRF Simulations. Model Domain: Covering the Area from 135 -105° W and 20 - 45° N. Horizontal Resolution: 30 km. Vertical Level: 28. Fu-Liou-Gu Radiation Scheme. Input: NCEP Final Analysis: Global, 1 Degree Resolution, Every 6 hours. 48-Hour Model Integration: Starting on March 29, 2007 at 0000 UTC.

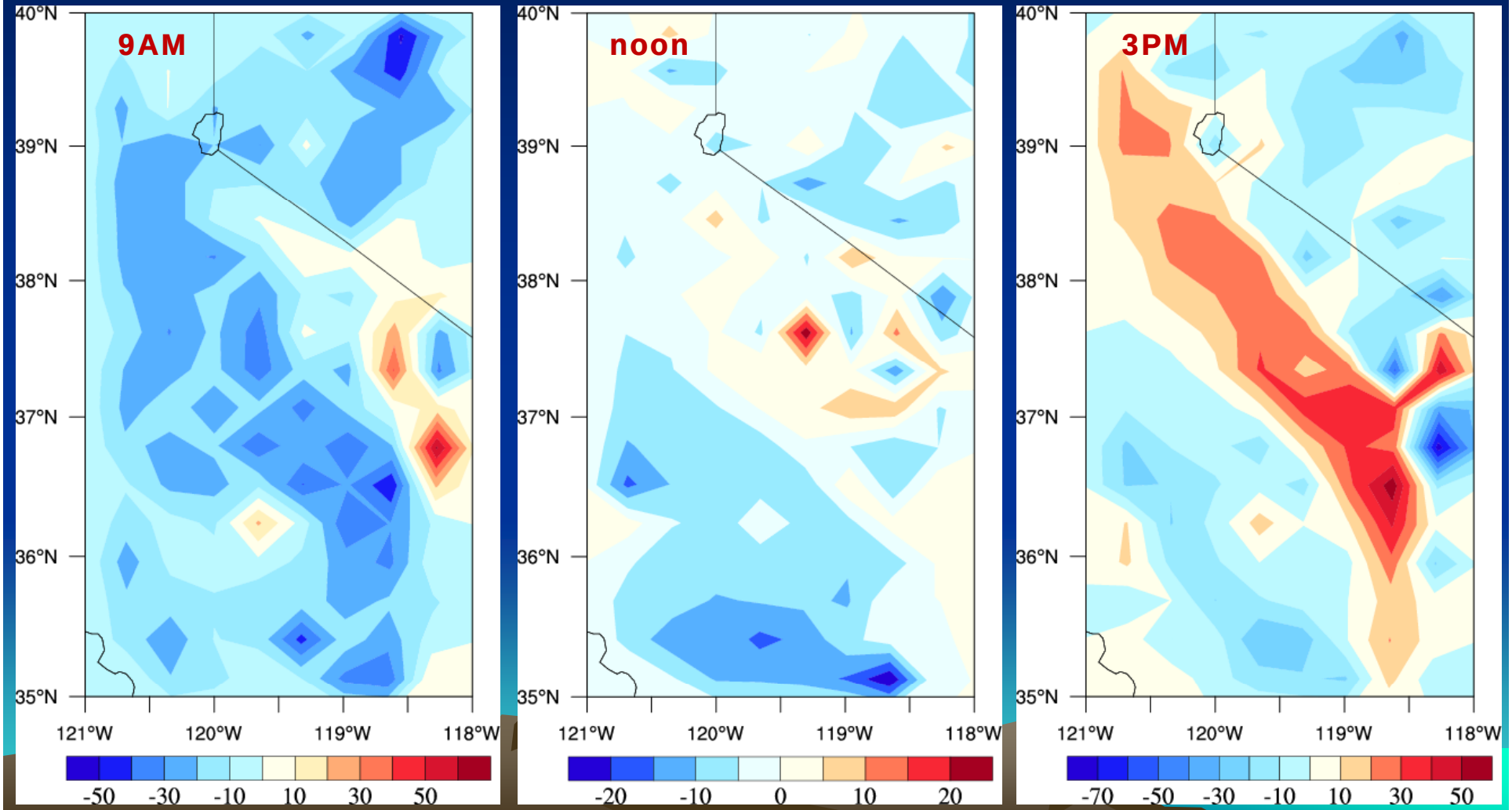

Differences in sensible and latent heat fluxes and surface temperature at 9 AM local time, March 29, 2007 in WRF simulations associated with the production of solar flux differences (3D-PP).

Sensible Heat Flux (W/m²) **Latent Heat Flux (W/m²)** **Surface Temperature (°C)**

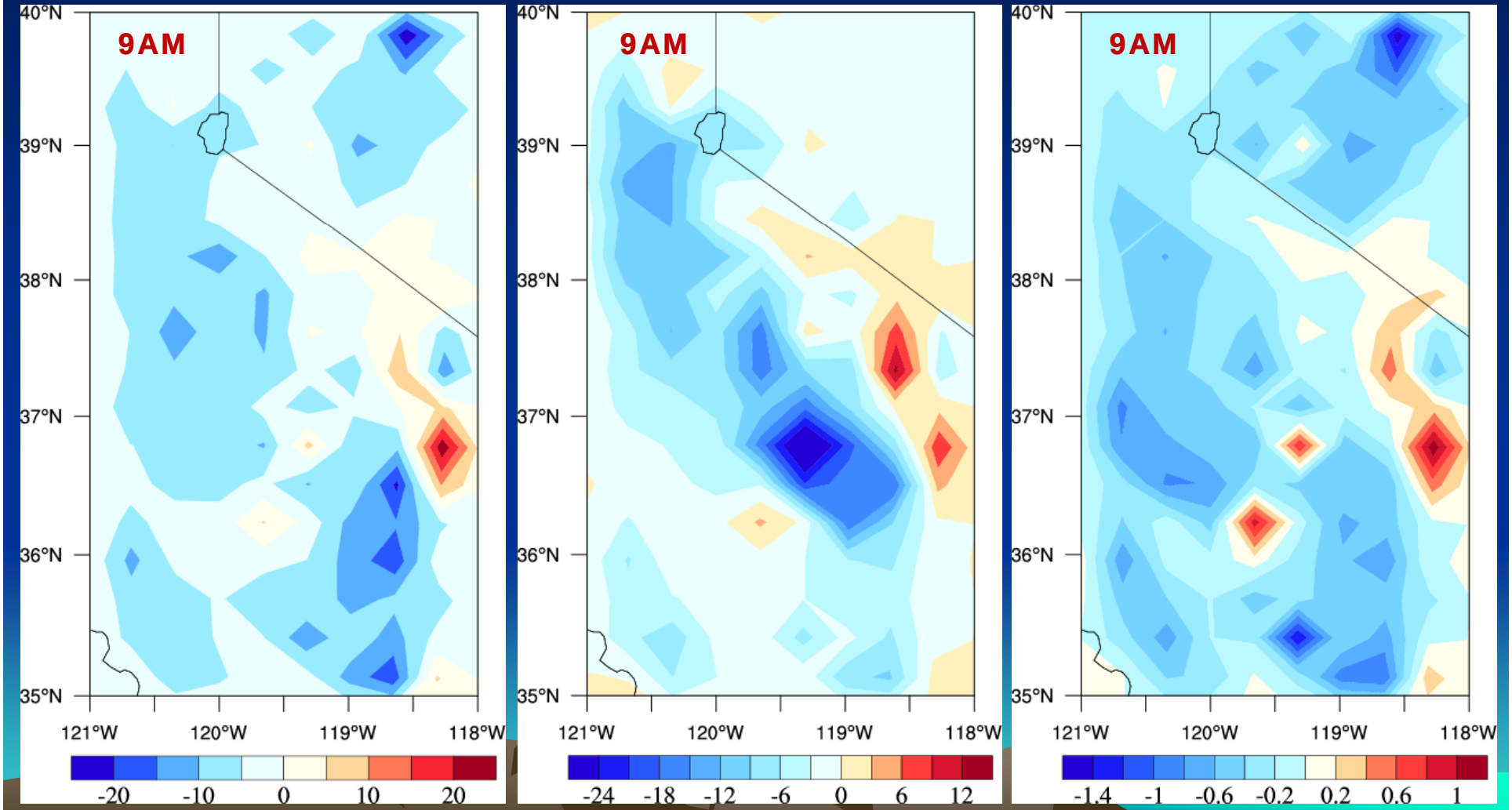

Connection to Surface Energy Balance Equation (Community Land Model, CLM <-> WRF)

Basic Equation

$$(\bar{S}_g + \bar{S}_v) + L^{\downarrow}_{\text{atm}} - L^{\uparrow} - (H_v + H_g) - (\lambda_{\text{vap}} E_v + \lambda E_g) = G$$

G = Ground Heat Flux $(= \partial T_S / \partial t)$

$(\bar{S}_g + \bar{S}_v)$ = Absorbed Solar Flux (v = vegetation, g = ground): 3D Effect

$L^{\downarrow}_{\text{atm}}$ = Incident Longwave Flux

$L^{\uparrow}$ = Emitted Longwave Flux

$(H_g + H_v)$ = Sensible Heat Flux

$(\lambda_{\text{vap}} E_v + \lambda E_g)$ = Latent Heat Flux (λ = certain coefficient)

3D Mountain Effects

$S_o(\text{3D}, \alpha)[1 - \alpha(\text{snow})]$; S_o = Incident Solar Flux, α = Snow Albedo

Solar Direct & Diffuse Beam (Visible & Near-IR): 3D Monte Carlo and Plane-Parallel Radiation Parameterizations

External & Internal Mixing of BC in Snow Grains

α(Grain Size, BC) = Snow Albedo: Optical Depth, Single-Scattering Albedo & Asymmetry Factor

An Illustration of Mountain/Snow-Albedo Feedback due to Absorbing Aerosols

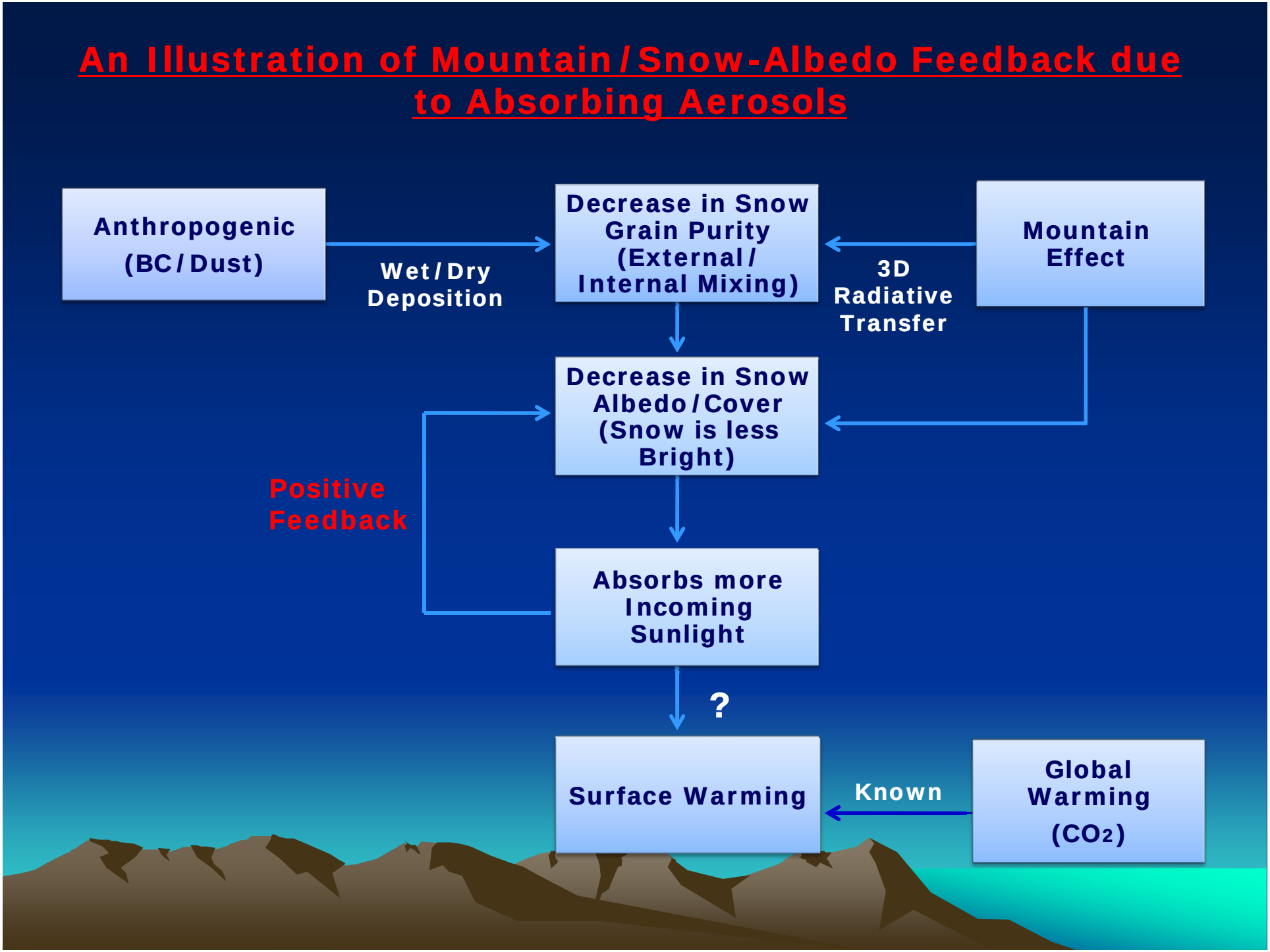

Human and Natural Drivers of Climate Change

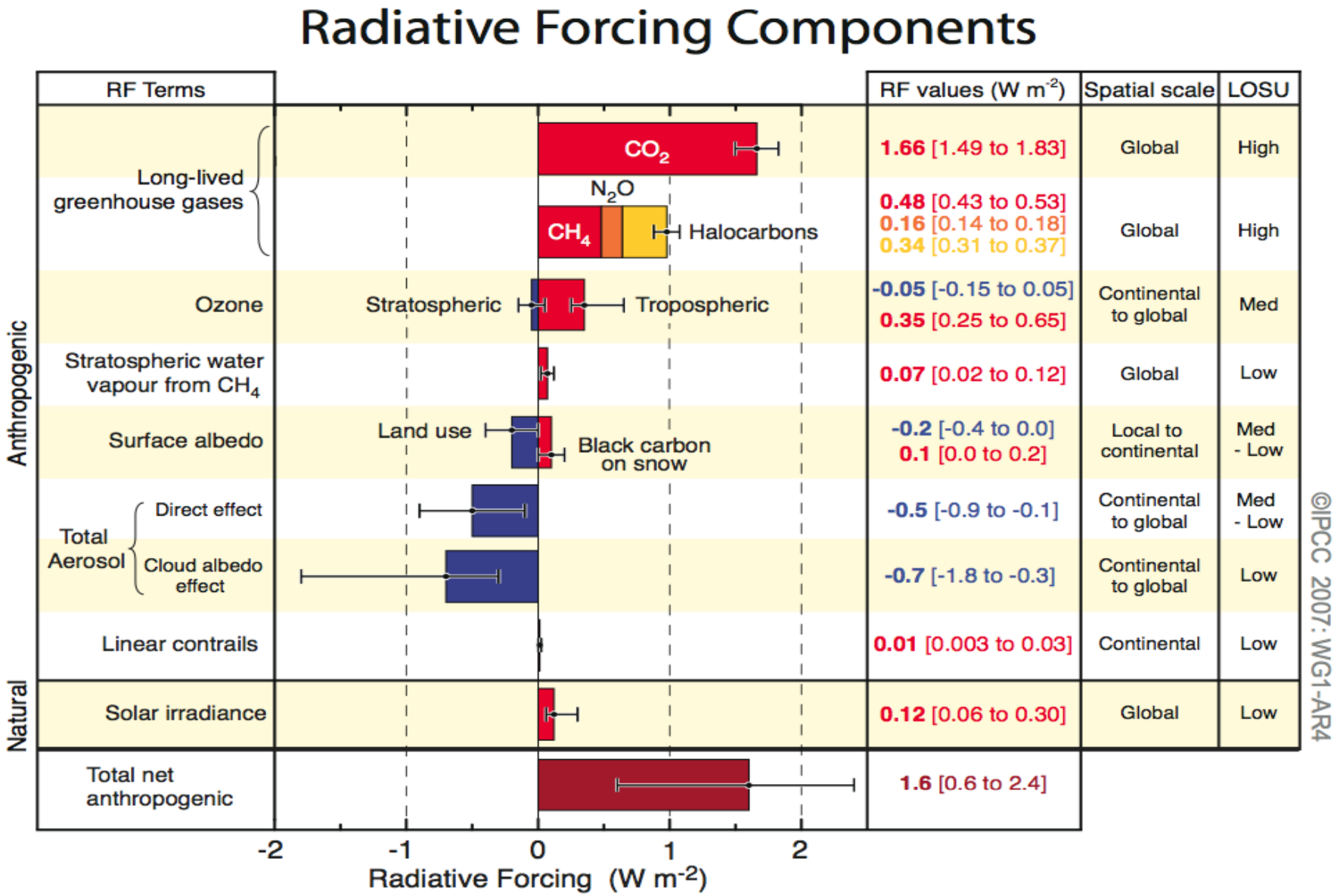

3D Mountain/Snow & Absorbing Aerosols: A Combined Regional Climate System

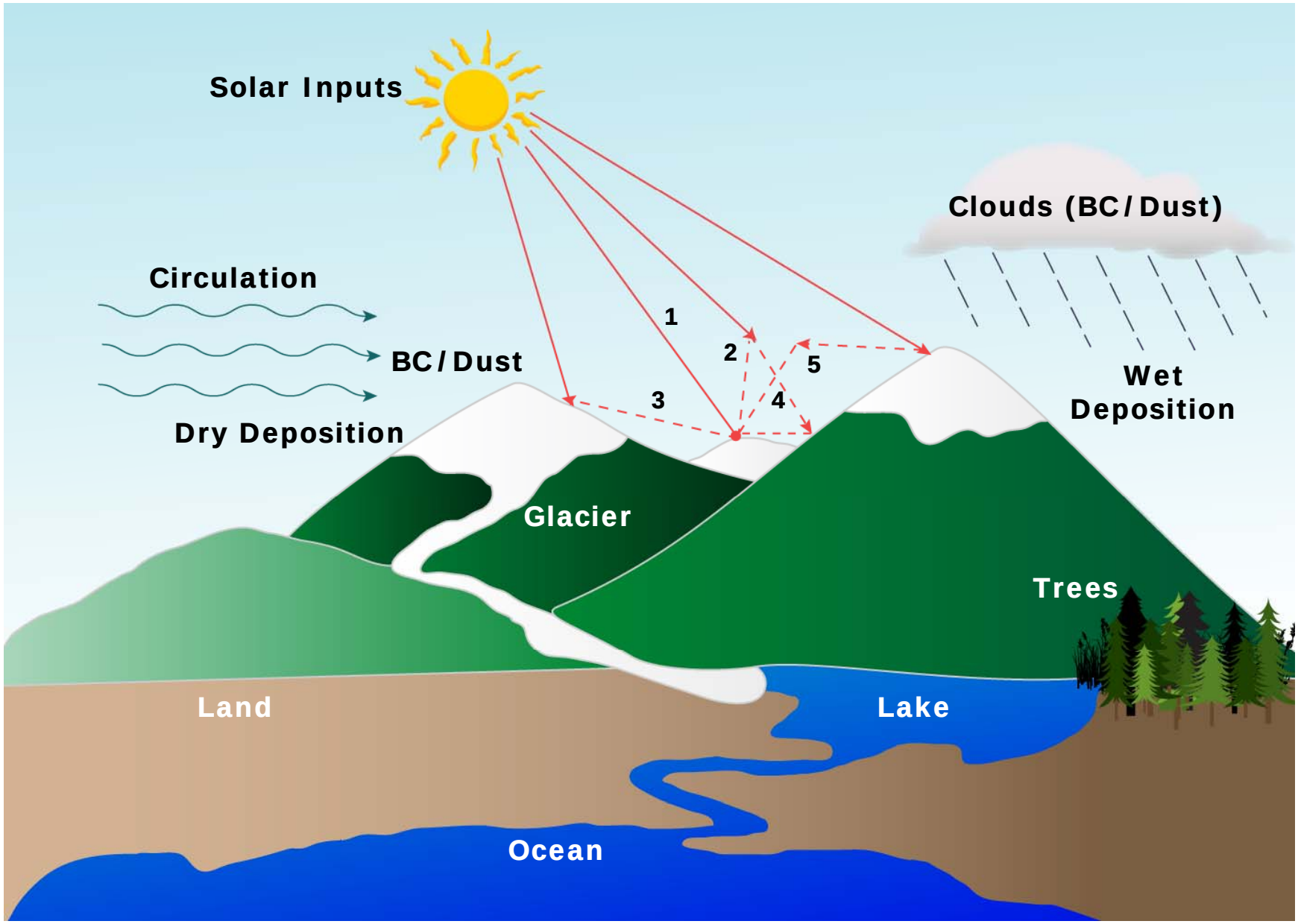

Radiative Transfer and Regional Climate Change: Some Remarks

- Two radiative transfer fundamentals, namely 3D radiative transfer over mountains/snow and light absorption of BC (soot) and dust, are critically important to understanding regional climate and climate change.
- Mountain snow albedo reduction appears to be linked to absorbing aerosols based on satellite data analysis over the Tibetan Plateau and the Sierras.
- Developed a 3D radiative transfer parameterization for surface solar fluxes in terms of deviations from PP results and successfully incorporated in WRF and CLM.
- Innovated a light absorption and scattering approach based on the principles of stochastic construction and geometric optics-surface wave integration for aggregates. Demonstrated the importance of internal mixing of BC in snow grains.
- On the concept of aerosols/mountain-snow/albedo feedback as a regional Earth system.

Radiative Transfer and Regional Climate Change: Award Lecture at the IRC Symposium, August 9, 2012, Berlin, Germany

Kuo-Nan Liou, University of California, Los Angeles, CA, USA

Mr. Chairman and distinguished colleagues, I am pleased to have the opportunity to present this lecture on the occasion of the IRC Gold Medal Award Ceremony. Radiative Transfer is an interdisciplinary subject and was studied principally by astrophysicists and later by planetary scientists and meteorologists for atmospheric applications. This field has also been an important research area in applied optics and mechanical and nuclear engineering.

Because the impact of radiative transfer in the atmosphere on dynamic processes takes time to be fully effective, it was generally assumed that its significance is more on climate, a time scale of perhaps more than a month, rather than weather forecast involving a few days. However, diurnal temperature variation is substantially controlled by solar and thermal infrared radiation, and the 4D assimilation of weather data for forecasting purposes requires a physically-based and efficient radiative transfer model.

The contemporary subject of the increase of carbon dioxide caused by man-made perturbations has been recognized to be a critical and irreversible factor contributing to climate change. We have now determined that absorption of thermal infrared radiation by CO2 in terms of line structure is the key to understanding its radiative forcing in the atmosphere and oceans and the subsequent increase in surface temperatures.

However, my talk will explore two radiative transfer issues that are specifically critical to regional climate and climate change: first, the issue of 3D radiative transfer in mountains/snow and second, absorbing aerosols within the context of a regional climate system. In particular, I would like to share with you my perspective on the importance of absorbing aerosols, specifically black carbon (BC or soot) and dust particles, in the reduction of snow albedo vis-a-vis aerosols-mountain snow-albedo feedback that would have an irreversible impact on regional climate and climate change (Slide 1).

*** For your entertainment, I have selected a number of slides (Slides 2-4) to illustrate the retreat of mountain snow in a number of locations, including the Kyetrak and Rongbuk Glaciers in Tibet, China; Mount Kilimanjaro in Tanzania; the Qori Kalis Glacier in Peru;**

and the Grinnell Glacier of Glacier National Park as well as the South Cascade glacier of Washington State in the United States. It appears quite evident that the reduction of mountain snow fields over the globe must be related to global warming. However, I would submit that the addition of man-made absorbing aerosols must also play a substantial role in this reduction in a non-linear fashion.

*** The global reduction of snow field can also be seen from Slide 5 taken from IPCC (2007). Panel (a) illustrates the NH March-April snow covered area obtained from ground-based and NOAA satellite datasets. The smooth curve shows decadal variations. Panel (b) shows differences in the distribution of NH M-A average snow cover between earlier (1967-1987) and later (1988-2004) portions of the satellite era. Yellow colors represent snow cover reduction. I have selected two specific areas: the Tibetan Plateau and the Sierra-Nevada Mountains, for my presentation. The Tibetan Plateau, with its mighty mountains, is considered to be the third pole of the Earth because of the vast amount of snow cover. The Sierra Nevada Mountains have substantial snow events in the winter and spring, representing important water resources not only for northern but also southern California. In fact, about 45% of S.C. water resources come from the Sierras.**

*** With respect to the Tibetan Plateau, Slide 6 illustrates the BC concentration determined at the Zuoqiupu Glacier from 1955-2005. Shown are annual and 5-year running mean results for monsoon, non-monsoon, and annual cases. The source of BC is primarily from the Indian subcontinent. Also shown in the middle and lower panels are corresponding surface air temperature and snow accumulation, respectively. It appears to demonstrate that the reduction in snow in that area is related to surface air temperature, as well as an increase in BC.**

*** This slide (slide 7) shows monthly averages of snow albedo for pixels with 100% snow cover, and associated land surface temperature and aerosol optical depth over the Tibetan Plateau in March and April from 2000 to 2010 taken from the MODIS data products. Error bars indicate one standard deviation. There appears to be a reasonable negative correlation between snow albedo and aerosol optical depth in this data.**

*** Slide 8a displays the BC (soot) concentration measured during the INDOX experiment, which was conducted in March 2001. The biomass burning in Southeast Asia and India have been identified and recognized as important source regions. Slide 8b shows**

the dust/aerosols originating in East Asia and China, as demonstrated in the 2001 perfect dust storm, using the aerosol optical depths determined from the TOMS instrument on board NOAA satellites to display the cross-Pacific transport of dust particles.

BC is produced by the incomplete combustion of carbonaceous fuels, including fossil fuel and biomass burning. China has been identified as a major global anthropogenic source for BC aerosols caused by its coal production and usage. Additionally, biomass burning in Southeast Asia and on the Indian subcontinent has also been noted as a substantial source of BC production. Dust production is directly related to regional weather systems over extremely dry regions; however, it can also be indirectly generated by man-made perturbations, such as deforestation and desertification.

*** In order to understand the transport of BC/dust aerosols from East Asia to the United States, we have analyzed the aerosol optical depths available from MODIS over the Sierra-Nevada Mountains, a region with snow cover in the winter season, for March and April, during a 10-year period. These results (Slide 9, only 4 years are shown) clearly illustrate the cross-Pacific transport of aerosols in general and BC/dust in particular from East Asia (source regions, red/yellow, 0.7 – 1 optical depths) to the Sierra-Nevada Mountains (green/light yellow, 0.3-0.5 optical depths). The selection of March-April is related to the aerosol activities in East Asia and the issue of snowmelt and water resources in California.**

*** In addition, we have run a simulation using a chemical transport model, referred to as GEOCHEM. This simulation (Slide 10) was conducted for the total aerosol optical depth in March and April for the year 2006; the results of this simulation reinforce the previous satellite aerosol optical depth observations. We need a chemical/aerosol transport model in order to quantify wet and dry depositions of absorbing aerosols onto the snow fields, a subject requiring further study.**

*** Over the Sierras, local emissions from industrial sites represent the primary sources of BC (~ 70%) that were observed. For illustration purposes, I have selected local sources using Los Angeles air pollution and the air pollution produced in Northern California as examples (Slide 11).**

*** Slide 12 displays a snow scene over the Sierra-Nevada Mountains in Northern California regions as well as three other mountain ranges: Tibet in China, the Alps in Europe, and the Rockies in America.**

*** Similar to the slide for the Tibetan Plateau presented earlier, I wanted to demonstrate that the lower snow albedo values in April compared to those in March over the Sierras are in part caused by absorbing aerosols transported from China and Southeast Asia. For this purpose, we analyzed the monthly mean and standard deviation of snow albedo (ranging from 0.5-0.8, Slide 13) and aerosol optical depth based on satellite observations. We showed that the snow albedo in April is consistently lower than in March, whereas the reverse is true for aerosol optical depth. Correlation analysis shows that these two parameters are negatively correlated with a high correlation coefficient and are statistically significant. I fully realize that snow albedo is also correlated with surface temperature in which the month of April is generally warmer than the month of March. Nevertheless, I would argue that the decrease in snow albedo with 100% snow cover in April, as compared with March is in part caused by the effect of absorbing BC and dust from East Asia.**

*** Why are BC and dust particles important in global radiative forcing and the climate system? The first reason is related to their direct radiative interactions with sunlight. The direct radiative forcing of BC/dust is determined by absorption and scattering processes and I have illustrated the physical connection of atmospheric absorption to vertical temperature profile, regional circulation, and regional surface temperature and precipitation on the right of this slide (Slide 14).**

*** Slide 15: I would like to present a GCM simulation to illustrate the significance of BC concentrations and the associated single-scattering albedo on the simulations of surface air temperature and precipitation. Using a single-scattering albedo of 0.88, a combination of 15% BC and 85% non-absorbing aerosols, we were able to reproduce the observed precipitation patterns in China, particularly over the Northwestern region, which in turn had the impact on the reduction of dust over the last 60 years.**

*** Dust particles are nonspherical and scatter and absorb sunlight, making the determination of their single-scattering properties a difficult issue in radiative transfer and remote sensing. Soot or BC particles are more complicated and some of them have fractal structures with respect to their morphology and composition (Slide 16). Soot is an aggregation of individual monomers, which can be structured in terms of internal and external mixing resulting in open and closed clusters or aggregations. These configurations lead to significant differences in their optical properties and the consequent single-**

scattering albedo value, important in climate study as shown in the previous GCM simulation.

*** Slide 17: In order to have a fundamental understanding of the radiative properties of BC, we must consider its basic geometric structure, size, composition, and optical properties. I shall now confine my presentation to radiative transfer in aerosols and focus specifically on black carbon. Soot or BC particles are complex with regards to their size, morphology, and composition. We have recently developed a new theoretical approach, which combines a stochastic process to build aggregates, followed by the geometric photon tracing including reflection/refraction, diffraction, and surface waves. The building block can be homogeneous or coated spheres with smooth or rough surfaces. We show an example of the stochastic process to construct aggregates that resemble their observed shape in the air. The light absorption and scattering program by small irregular particles based on the geometric-optics and surface-wave approach has been verified by comparison with existing results for columns and plates. The next 3 slides show some representative results.**

*** Slide 18 illustrates substantial differences between realistic aggregate shapes and commonly assumed spheres in terms of reflection, absorption, and transmission for typical BC sizes of 0.03 (and 0.07 □m) as a function of aerosol mass path. Because of their irregular shapes, the optical depth can be determined from mass extinction coefficient and aerosol mass path. Aggregates reflect and absorb more light than their spherical counterparts. Spheres are not a good approximation for BC in radiative transfer calculations.**

*** Slide 19: In the following slide, we illustrate the importance of the contamination of snow grains by absorbing aerosols. Internal mixing produces much larger absorption, as compared with its external counterpart, in terms of a larger single-scattering co-albedo. The subsequent radiative transfer calculations illustrate reduction of snow albedo associated with the contamination of BC and dust particles, depending on their size. Due to its larger absorption, BC has a more substantial impact than dust particles do on the reduction of snow albedo. A 1-□m sized soot particle internally mixed with snow grains could effectively reduce snow albedo by as much as 5-10 %.**

*** Slide 20: Spectral single-scattering co-albedo, asymmetry factor, and snow albedo**

results for snow grains externally and internally mixed with 3 soot sizes to illustrate the importance of internal mixing in snow grains in reducing the single-scattering albedo value and the consequence of snow albedo based on simple radiative transfer calculations. Also shown is the effect of the snow grain's irregular shape on the reduction of the asymmetry factor and hence the forward scattering power, as compared to the spherical counterpart. The information content in this figure is quite rich at the fundamental level; however, in the interest of time I shall move on to 3D radiative transfer in mountains/snow.

*** Slide 21: It appears unlikely that analytical solutions, such as 2-stream, Eddington, and 4-stream approximations for radiative transfer, can be derived for intricate mountains/snow fields. In my opinion, the only solution is by means of the Monte Carlo simulation, which can be applied to any geometry, but unfortunately, formidable computational efforts are required to achieve reliable accuracy. We have made substantial advances in modeling the transfer of solar and thermal IR radiation involving intense topography following Monte Carlo photon tracing. The transfer of solar radiation is composed of 5 components- direct, diffuse, direct-reflected, diffuse-reflected, and coupled fluxes- related to the solar incident angle, elevation, sky view factor, and terrain configuration factor.**

*** This Slide (22) displays a comparison of the deviations (from plane-parallel results) of the five flux components computed from Monte Carlo simulations (real values) and multiple regression equations (predicted values) using a domain of 10 km. The upper panel displays direct and diffuse fluxes. The middle panel is for direct-reflected and diffuse-reflected fluxes. The lower panel shows the coupled flux with a surface albedo of 0.1 and 0.7. The most important component is direct flux (~ 700 W/m^2), followed by direct-reflected flux. We have derived 5 universal regression equations for flux deviations which have the general linear form for the 5 flux components, as shown in the lower panel. For example, for the deviation of direct flux, F^*_{dir}, we have $a_1 + b_{11}\, y_1 + b_{12}\, y_2$, where y_1 is the mean cosine of the solar zenith angle, y_2 is the mean sky view factor, and b_{11} and b_{12} are regression coefficients. This parameterization is applicable to clear as well as cloudy conditions using cloud optical depth as a scaling factor. The flux deviation results can be directly added to the existing surface radiative flux values determined from a land-surface model to account for 3D mountain effects.**

*** We have successfully incorporated the preceding 3D radiative transfer parameterization in the Weather Research and Forecasting (WRF) Model using the Sierra-Nevada Mountains in the Western United States as a testbed. Slide 23 illustrates this region's elevation and slope.**

*** The next slide (24) shows solar flux differences (3D-PP) for March 29, 2007 in WRF simulations for a 2-day model integration. The domain is over the Western U.S. with a horizontal resolution of 30 km and 26 vertical levels. The input parameters are from the NCEP Final Analysis. Substantial flux deviations are displayed for 9AM, noon, and 3PM local times, the patterns of which are dependent on the sun's position with respect to mountain orientation.**

*** Increases and decreases in surface solar fluxes will affect surface processes. Slide 25 illustrates the induced changes in sensible heat fluxes, which range from about -20 to +20 W/m2. A similar range is seen for latent heat fluxes. As a result, surface temperature displays increases in the sunny side and reductions in the shaded side in comparison to the control run using a PP radiative transfer model. Recent results from a one-month WRF simulation show similar patterns for the surface heat components.**

*** Slide 26 depicts the components of surface energy budget in the Community Land Model (CLM) developed in NCAR, including terms associated with vegetation. The effects of 3D radiative transfer over mountains and snow grain contamination on surface processes are both related to the albedo term. We would like to use CLM and perhaps a simplified surface model to understand and quantify feedback processes outlined in the next slide.**

*** Slide 27 demonstrates the essence of snow-albedo feedback, a powerful amplification process involving absorbing aerosols. Through the wet and/or direct dry deposition of absorbing aerosols, snow becomes less bright. As a consequence, it will absorb more incoming sunlight, leading to surface warming. The loop involving darker snow and absorbing more sunlight forms a powerful feedback mechanism that can significantly amplify surface temperature increase. In conjunction with this, we have witnessed powerful ice-albedo feedback in the Arctic and Antarctic regions. However, we need to quantify the surface warming produced by dry and wet depositions. Also, we need to quantify the 3D mountain radiative effect in a model setting on the state of snow albedo with reference to**

the conventional PP radiation program.

*** Slide 29is the well-known IPCC chart for the global radiative forcings estimate produced by natural and human disturbances of climate change, including greenhouse gases, aerosols, and other forcing elements. Globally, BC on snow is shown to have only a small value; however, this forcing must be much more substantial in the regional context, particularly if the powerful feedback processes have been properly included and accounted for.**

*** Our conceptual approach for regional climate modeling is illustrated in Slide 29, which displays a graphic depiction of the effect of 3D mountain/snow and absorbing aerosols via dry and wet deposition with respect to the solar inputs as a combined regional climate system.**

*** Slide 30: Summary remarks. I have demonstrated that (1) two radiative transfer fundamentals: 3D radiative transfer over mountains/snow and light absorption of BC (soot) and dust, are critically important to understanding regional climate and climate change and (2) presented some evidence of mountain snow albedo reduction linked to absorbing aerosols based on satellite data analysis over the Tibetan Plateau and the Sierras. Secondly, we have (3) developed a 3D radiative transfer parameterization for surface solar fluxes in terms of deviations from PP results and successfully incorporated in WRF and CLM, and (4) innovated a light absorption and scattering approach based on the principles of stochastic processes and geometric optics-surface wave integration for aggregates and demonstrated the importance of internal mixing of BC in snow grains. Finally, I have presented the concept of aerosols/mountain-snow/albedo feedback as a regional Earth system in association with radiative transfer.**